



**ROBUST H_∞ SAMPLED-DATA SLIDING MODE CONTROL FOR
MARKOV SWITCHING STOCHASTIC NEUTRAL-TYPE
SYSTEMS WITH MIXED DELAYS AND LÉVY NOISES**

JAYASRI DHANDAPANI^{✉1}, ANBAZHAGAN NEELAMEGAM^{✉1},
VADIVEL RAJARATHINAM^{✉2}, MOSTAFA FAZLY^{✉*3}
AND NALLAPPAN GUNASEKARAN^{✉*4}

¹Department of Mathematics, Alagappa University, Karaikudi,
630003, Tamil Nadu, India

²Department of Mathematics, Faculty of Science and Technology,
Phuket Rajabhat University, Phuket, 83000, Thailand

³Department of Mathematics, University of Texas at San Antonio,
San Antonio, TX 78249, United States of America

⁴Eastern Michigan Joint College of Engineering, Beibu Gulf University,
Qinzhou 535011, Guangxi, China

(Communicated by Tuoc Phan)

ABSTRACT. This paper examines the control problem of stochastic neutral-type systems (SNTSs) that experience parameter uncertainties, mixed delays, external disturbances, and Lévy noises under Markovian switching. To address this problem, an appropriate Lyapunov-Krasovskii functional (LKF) is formulated, and the generalized Itô formula is used in conjunction with inequality techniques to establish exponential stability and guarantee H_∞ performance. The primary objective is to achieve exponential stabilization of SNTSs using a sampled-data sliding mode control (SDSMC) strategy designed using linear matrix inequalities (LMIs). An integral sliding surface is introduced, and the corresponding equivalent control is derived to ensure the stability of the systems. Subsequently, a sliding mode control law was developed to guarantee both the existence of the sliding mode and the reachability of the switching surface. Finally, numerical simulations are presented to demonstrate the validity and robustness of the proposed control approach.

1. Introduction. Extensive research has focused on stochastic differential equations due to their broad applicability in engineering, and many important results concerning these systems have been addressed in the existing literature [20, 26, 40, 18]. The behavior of many systems is influenced by their past states, making neutral-type equations essential for modeling real-world dynamics. These equations incorporate both state delays and their derivatives, making them particularly relevant in various scientific and engineering applications, such as heat conduction

2020 *Mathematics Subject Classification.* Primary: 93D05, 34K50, 60H10; Secondary: 35B35, 34K20.

Key words and phrases. Stochastic neutral-type systems, sampled-data sliding mode control, Lyapunov stability, Lévy noises, mixed delays.

*Corresponding authors: Mostafa Fazly, Nallappan Gunasekaran.

systems, microwave oscillator circuits, and models of population dynamics. Due to their extensive practical relevance, the evaluation of their stability and synchronization control for neutral-type systems has received considerable interest from researchers in recent years [6, 25, 29, 2]. For example, in [25], neural network-based passive filtering was studied for delayed neutral-type systems that exhibit stochastic and Markovian switching behavior. Furthermore, in [2], stability estimates for neutral-type systems with distributed time-varying delays were studied using Lyapunov-Krasovskii functional (LKF) and integral inequality techniques. Real-world systems frequently encounter abrupt parameter variations that may arise from subsystem interactions or unexpected component malfunctions. Such sudden changes can be effectively modeled using Markovian switching frameworks, in which a Markov chain is employed to characterize the probabilistic transitions among different operating modes of the system. Due to their strong applicability to capture dynamic parameter shifts and mode-dependent behaviors, Markovian switching systems have become an important focus of research in modern control theory [15, 17, 10, 9]. In [10], synchronization conditions were derived for neutral-type neural networks with Markovian jump parameters and time-varying delays based on Lyapunov stability theory and event-triggered mechanisms. Similarly, in [9], a stabilization criterion was established for stochastic neutral-type systems (SNTSs) with Markovian switching using the linear matrix inequalities (LMIs) method.

Recently, stability analysis has been widely discussed in the literature [34, 28, 3]. In particular, a new global asymptotic stability approach for bidirectional associative memory neural networks was presented in [28]. Lévy noises, a stochastic process that incorporates continuous and jump components, frequently appears in financial modeling and statistical applications [7, 42, 37, 16, 41, 44, 46]. In [16], we study stochastic fixed-time synchronization of delayed neural networks affected by Lévy noises using a Lyapunov-based approach. Furthermore, in [44], an adaptive control-based synchronization strategy was introduced to guaranty the stable behavior of the Master–Slave system, where dynamic parameters and control gains were systematically determined. Recent work, [46] studies simple event-triggered sampling methods that ensure exponential stability of stochastic nonlinear delay systems affected by Lévy noises.

Sliding mode control (SMC) is a widely utilized method for controlling SNTSs, valued for its quick response and robustness against parameter variations and external disturbances. The SMC consists of two primary processes: the reaching phase, where the state of the system approaches the sliding mode surface (SMS), and the sliding phase, where the system dynamics evolve along the designed switching surface. Once on the switching surface, the system remains insensitive to uncertainties and disturbances. The effectiveness of SMC has been demonstrated in various non-linear systems [23, 24, 1, 31]. In [24], we studied how Markovian control can be applied to nonlinear stochastic switching systems with quantization constraints. Similarly, in [1], adaptive fixed-time SMC has been used to quickly and reliably control nonlinear systems despite uncertainties. This method ensures fast convergence independent of initial conditions.

However, the digital modeling of continuous control systems also requires the discretization process as a crucial step. Consequently, the study of sampling data control has gained significant attention, as implementing sampling control enhances the control precision and resistance of the system’s to interference. In addition, it contributes to better utilization and adaptability of the controller. Recently,

event-triggered and aperiodic sampled-data control strategies have been proposed for stochastic systems to further reduce communication and computation burden while ensuring exponential stability [35, 36]. On the other hand, sampled-data sliding mode control (SDSMC) have been thoroughly researched for various kinds of systems [4, 5, 32, 21]. Including Markovian jump complex network systems [13], chaotic systems [39], complex dynamical networks [33, 38], and neural networks [11]. In this study, sampling is incorporated into the SMC framework. Inspired by these findings, this study introduces a novel SDSMC strategy to achieve exponential stability in SNTSs under Lévy noises. The key contributions of this work include:

- (i) Incorporating Lévy noises into the SNTSs framework to capture real-world disturbances more accurately.
- (ii) A new LKF is constructed, which explicitly incorporates the discrete sampling instants t_p, t_{p+1} and employs integral inequalities such as Jensen's, Young's, and Newton-Leibniz formula to reduce conservatism. Based on this, the exponential stability conditions are established in terms of LMIs.
- (iii) Designing an adaptive SDSMC law is proposed to ensure the existence of the sliding mode and the reachability of the sliding surface while guaranteeing the desired system performance. The feasibility of the LMI-based conditions is validated through numerical examples using MATLAB simulations.

Notations: \mathbb{R}^n denotes the Euclidean space of dimension n , $\mathbb{R}^{n \times m}$ represents the set of all real matrices of size $n \times m$. The notation \mathcal{A}^T stands for the transpose of a matrix \mathcal{A} , while \mathcal{A}^{-1} denotes its inverse. The symbol $*$ indicates elements determined by symmetry. The Euclidean norm is represented by $\|\cdot\|$. A matrix $\mathcal{A} > 0$ means that \mathcal{A} is real, symmetric, and positive definite. The operator \mathbb{E} denotes the expectation and $\mathcal{L}_2[0, \infty)$ refers to the space of square-integrable vector functions on $[0, \infty)$.

Let $\{\hat{q}(t), t \geq 0\}$ represent a right-continuous Markov process [43, 14] defined on the finite state space $\mathbb{S} = \{1, 2, \dots, N\}$. The evolution of this process is characterized by the transition rate matrix $\Gamma = (\pi_{lj})$, whose elements satisfy

$$\mathbf{Prob}\{\hat{q}(t + \Delta) = j \mid \hat{q}(t) = l\} = \begin{cases} \pi_{lj}\Delta + o(\Delta), & l \neq j, \\ 1 + \pi_{ll}\Delta + o(\Delta), & l = j, \end{cases}$$

where $\pi_{lj} \geq 0$ for all $l \neq j$, and condition $\sum_{j=1}^{j=N} \pi_{lj} = 0$ is satisfied.

2. Preliminaries and system description. Let us consider the SNTSs with mixed delays, uncertainties, and Lévy noises with Markov switching:

$$\begin{aligned} d[\hat{\delta}(t) - \hat{A}(\hat{q}(t))\hat{\delta}(t - \tau)] = & \left\{ (\hat{B}(\hat{q}(t)) + \Delta\hat{B}(\hat{q}(t)))\hat{\delta}(t) + (\hat{C}(\hat{q}(t)) \right. \\ & + \Delta\hat{C}(\hat{q}(t)))\hat{\delta}(t - \eta(t)) + \hat{D}(\hat{q}(t))(\hat{u}(t) \\ & + \hat{f}(\hat{\delta}(t), \hat{\delta}(t - \eta(t)), t) + \hat{E}(\hat{q}(t))\hat{w}(t)) \Big\} dt \quad (1) \\ & + \mathcal{B}_1(t)(\hat{q}(t))\tilde{\sigma}(\hat{\delta}(t), \hat{\delta}(t - \eta(t)), \hat{q}(t))d\mathcal{B}(t) \\ & + \mathcal{B}_2(t)(\hat{q}(t)) \int_{\mathbb{R}} \hat{\mu}(\hat{\delta}(t), \hat{\delta}(t - \eta(t)), \hat{q}(t), y) \\ & \hat{N}(dt, dy), \\ \hat{z}(t) = & \hat{G}(\hat{q}(t))\hat{\delta}(t) + \hat{H}(\hat{q}(t))\hat{w}(t), \end{aligned}$$

where $\hat{\delta}(t) \in \mathbb{R}^n$ denotes the system state vector, $\hat{u}(t) \in \mathbb{R}^m$ the control input, and $\hat{w}(t) \in \mathbb{R}^m$ is the exogenous disturbance belonging to the space $\mathcal{L}_2[0, \infty)$. The system output is represented by $\hat{z}(t) \in \mathbb{R}^m$, the unknown nonlinear function $\hat{f}(\cdot)$ belongs to \mathbb{R}^m , and the stochastic behavior is influenced by the Brownian motion $\mathcal{B}(t) \in \mathbb{R}^m$. The matrices $\hat{A}(\hat{\rho}(t)) \in \mathbb{R}^{n \times n}$, $\hat{B}(\hat{\rho}(t)) \in \mathbb{R}^{n \times n}$, $\hat{C}(\hat{\rho}(t)) \in \mathbb{R}^{n \times n}$, $\hat{D}(\hat{\rho}(t)) \in \mathbb{R}^{n \times m}$, $\hat{E}(\hat{\rho}(t)) \in \mathbb{R}^{n \times m}$, and $\mathcal{B}_1(\hat{\rho}(t)), \mathcal{B}_2(\hat{\rho}(t)) \in \mathbb{R}^{n \times n}$ are fixed system parameters. The terms $\Delta\hat{B}(\hat{\rho}(t))$ and $\Delta\hat{C}(\hat{\rho}(t)) \in \mathbb{R}^{n \times n}$ are time-varying matrices that contain bounded uncertainties. These uncertainties take the forms $\Delta\hat{B}(\hat{\rho}(t)) = \hat{L}F(\hat{\rho}(t), t)\hat{J}_a$ and $\Delta\hat{C}(\hat{\rho}(t)) = \hat{L}F(\hat{\rho}(t), t)\hat{J}_b$, where \hat{L} , \hat{J}_a , \hat{J}_b are known matrices, and $F(\hat{\rho}(t), t)$ is an unknown time-varying matrix satisfying $F^T(\hat{\rho}(t), t)F(\hat{\rho}(t), t) \leq I$. The diffusion term is characterized by the noise intensity matrix $\tilde{\sigma}$ belonging to $\mathbb{R}^n \times \mathbb{R}^n \times \mathbb{S} \rightarrow \mathbb{R}^{n \times m}$. A Poisson random measure \hat{N} is defined in $\mathbb{R}_+ \times (\mathbb{R}^d - \{0\})$ with a compensator \tilde{N} and a Lévy measure ν satisfying $\tilde{N}(dt, dy) = \hat{N}(dt, dy) - \nu(dy)dt$, $\int_{\mathbb{R}^n - \{0\}} (|y|^2 \wedge 1) \nu(dy) < \infty$. The matrices $\hat{G} \in \mathbb{R}^{n \times m}$ and $\hat{H} \in \mathbb{R}^{n \times m}$ are constants, and $\hat{\mu} : \mathbb{R}^d \times \mathbb{R}^d \times \mathbb{R}^d \rightarrow \mathbb{R}^d$ defines the jump function. The system involves both a constant delay τ and a time-varying delay $\eta(t)$ that satisfy the constraints $0 \leq \eta(t) \leq \bar{\eta}$, $\dot{\eta}(t) \leq \hat{\eta} < 1$, $\forall t \geq 0$, and $\hat{\eta} > 0$. The maximum delay is given by $d = \max\{\tau, \bar{\eta}\}$.

Remark 2.1. Unlike [29, 15, 17], the model (1) makes effective use of Lévy noises to simulate different types of disturbances and interferences. Lévy noises capture both continuous and discontinuous fluctuations, combining the strengths of Brownian motion and Poisson point processes. This dual advantage allows Lévy noises to more accurately represent real-world noise, making them a more suitable choice than using Brownian motion or Poisson point processes alone.

For simplicity, we introduce the following notation: let $\hat{\rho}(t) = i$, $\hat{\delta}(t - \tau) = \hat{\delta}_\tau(t)$, and $\hat{\delta}(t - \eta(t)) = \hat{\delta}_\eta(t)$. Define $\hat{f}(\hat{\delta}(t), \hat{\delta}(t - \eta(t)), t) = \hat{f}(t)$, $\hat{C}(\hat{\rho}(t)) = \hat{C}_i$, $\hat{A}(\hat{\rho}(t)) = \hat{A}_i$, $\hat{B}(\hat{\rho}(t)) = \hat{B}_i$, $\hat{D}(\hat{\rho}(t)) = \hat{D}_i$, and $\hat{E}(\hat{\rho}(t)) = \hat{E}_i$. Similarly, set $\mathcal{B}_1(\hat{\rho}(t)) = \mathcal{B}_{1i}$, $\mathcal{B}_2(\hat{\rho}(t)) = \mathcal{B}_{2i}$, $\Delta\hat{C}(\hat{\rho}(t), t) = \Delta\hat{C}_i$, and $\Delta\hat{B}(\hat{\rho}(t), t) = \Delta\hat{B}_i$. In addition, denote $\tilde{\sigma}(\hat{\delta}(t), \hat{\delta}(t - \eta(t))) = \tilde{\sigma}_i$, $\hat{\mu}(\hat{\delta}(t), \hat{\delta}(t - \eta(t)), \hat{\rho}(t), i, y) = \hat{\mu}_i$, $\hat{G}(\hat{\rho}(t)) = \hat{G}_i$, and $\hat{H}(\hat{\rho}(t)) = \hat{H}_i$.

Therefore, the system in equation (1) can be rewritten as follows:

$$\begin{aligned} d[\hat{\delta}(t) - \hat{A}_i \hat{\delta}_\tau(t)] &= \left\{ (\hat{B}_i + \Delta\hat{B}_i) \hat{\delta}(t) + (\hat{C}_i + \Delta\hat{C}_i) \hat{\delta}_\eta(t) + \hat{D}_i (\hat{u}(t) + \hat{f}(t)) \right. \\ &\quad \left. + \hat{E}_i \hat{w}(t) \right\} dt + \mathcal{B}_{1i}(t) \tilde{\sigma}_i d\mathcal{B}(t) + \mathcal{B}_{2i}(t) \int_{\mathbb{R}} \hat{\mu}_i \hat{N}(dt, dy), \\ \hat{\delta}(t) &= \tilde{\Xi}(t), \quad \forall t \in [-d, 0]. \end{aligned} \quad (2)$$

The essential concepts, supporting lemmas, and stability assumptions are presented here.

Lemma 2.2. [27] *Let Ω , \hat{L} , and \hat{E} be given matrices, and assume that F is a function satisfying $F^T F \leq I$. Then, the inequality $\Omega + \hat{L}F\hat{E} + [\hat{L}F\hat{E}]^T \leq 0$ holds if and only if there exists a scalar $\alpha \geq 0$ that satisfies $\Omega + \alpha^{-1}\hat{L}^T\hat{L} + \alpha\hat{J}^T\hat{J} < 0$.*

Lemma 2.3. [19] *Let $P \in \mathbb{R}^{n \times n}$ be a symmetric matrix such that $P = P^T$, and let $\tau > 0$ be a scalar. For a vector function $\varpi(s) \in \mathbb{R}^n$, assuming that the integral*

involved is well-defined, the following inequality holds:

$$-\int_{t-\tau}^t \varpi^T(s)P\varpi(s)ds \leq \frac{-1}{\tau} \left(\int_{t-\tau}^t \varpi(s)ds \right)^T P \left(\int_{t-\tau}^t \varpi(s)ds \right).$$

Lemma 2.4. [19] For any matrices $\tilde{X}, \tilde{Y} \in \mathbb{R}^n$, matrix $\tilde{Q} > 0$, the following inequality is established:

$$2\tilde{X}^T\tilde{Y} \leq \tilde{X}^T\tilde{Q}\tilde{X} + \tilde{Y}^T\tilde{Q}^{-1}\tilde{Y}.$$

Lemma 2.5. [19] Given constant matrices $\tilde{X} = \tilde{X}^T$ and $\tilde{Y} = \tilde{Y}^T$. If $\begin{bmatrix} \tilde{X} & \tilde{Z} \\ \tilde{Z}^T & \tilde{Y} \end{bmatrix} > 0$, then it leads to the conditions

$$\tilde{X} > 0, \quad \tilde{Y} - \tilde{Z}^T\tilde{X}^{-1}\tilde{Z} > 0,$$

or

$$\tilde{Y} > 0, \quad \tilde{X} - \tilde{Z}\tilde{Y}^{-1}\tilde{Z}^T > 0.$$

Lemma 2.6. [45] Let C_1^2 represent the class of nonnegative functions $V(t, \hat{\delta})$ defined on $\mathbb{R}_+ \times \mathbb{R}^d$, which are twice continuously differentiable with respect to $\hat{\delta}$ and continuously differentiable in t . If $V(t, \hat{\delta}(t)) \in C_1^2(\mathbb{R}_+ \times \mathbb{R}^d; \mathbb{R}_+)$ then an operator $\mathcal{I}\hat{\delta}$ from $\mathbb{R}_+ \times \mathbb{R}^d$ to \mathbb{R} can be expressed as

$$\begin{aligned} \mathcal{L}V(t, \hat{\delta}(t)) &= V_t(t, \hat{\delta}(t)) + V_{\hat{\delta}}(t, \hat{\delta}(t))f(\hat{\delta}(t)) \\ &\quad + \frac{1}{2} \text{trace}[g^T(\hat{\delta}(t))V_{\hat{\delta}\hat{\delta}}(t, \hat{\delta}(t))g(\hat{\delta}(t))] \\ &\quad + \int_{|y|<c} [V(t, \hat{\delta}(t) + \hat{\mu}(\hat{\delta}(t), y)) - V(t, \hat{\delta}(t)) \\ &\quad - \hat{\mu}(\hat{\delta}(t), y)V_{\hat{\delta}}(t, \hat{\delta}(t))] \nu(dy), \end{aligned}$$

where $V_t(t, \hat{\delta}(t)) = \frac{\partial V(t, \hat{\delta}(t))}{\partial t}$, $V_{\hat{\delta}}(t, \hat{\delta}(t)) = \left(\frac{\partial V(t, \hat{\delta}(t))}{\partial \hat{\delta}_1}, \dots, \frac{\partial V(t, \hat{\delta}(t))}{\partial \hat{\delta}_n} \right)$, $V_{\hat{\delta}\hat{\delta}}(t, \hat{\delta}(t)) = \left(\frac{\partial^2 V(t, \hat{\delta}(t))}{\partial \hat{\delta}_i \partial \hat{\delta}_j} \right)_{(n \times n)}$.

Definition 2.7. [8] Consider the system (2) with the initial condition $\tilde{\Xi} \in \mathbb{L}_{\mathcal{F}_0}^2([-d, 0], \mathbb{R}^n)$. The system is said to be second-moment exponentially stable if

$$\lim_{T \rightarrow \infty} \mathbb{E} \int_0^T \left\| \hat{\delta}(t; \tilde{\Xi}(0), \hat{\varrho}(0)) \right\|^2 dt < \infty.$$

Definition 2.8. [12] The dynamical system (7) is said to be stochastically stable with a specified disturbance attenuation level $\gamma > 0$, if it remains stochastically stable under zero initial conditions and satisfies

$$\|\hat{z}(t)\|_2 \leq \|\hat{w}(t)\|_2,$$

for every non-zero $\hat{w}(t) \in \mathcal{L}_2[0, \infty)$.

Assumption 2.9. [19] There exists a positive constant k , for any $\hat{\delta} \in \mathbb{R}^n, \tilde{q} > 0$ such that

$$\int_{\mathbb{R}} |\hat{\mu}(\hat{\delta}, y)|^{\tilde{q}} \nu(dy) \leq k |\hat{\delta}|^{\tilde{q}}.$$

Assumption 2.10. [8] *The noise intensity matrix $\tilde{\sigma}(t, \hat{\delta}(t), \hat{\delta}(t - \eta(t)))$ satisfies*

$$\begin{aligned} & \text{trace}[\tilde{\sigma}^T(t, \hat{\delta}(t), \hat{\delta}(t - \eta(t)))\mathcal{B}_{1i}^T\mathcal{B}_{1i}\tilde{\sigma}(t, \hat{\delta}(t), \hat{\delta}(t - \eta(t)))] \\ & \leq \hat{\delta}^T(t)x_{i1}\hat{\delta}(t) + \hat{\delta}^T(t - \eta)x_{i2}\hat{\delta}(t - \eta), \end{aligned}$$

where $x_{i1} \geq 0$ and $x_{i2} \geq 0$ are real matrices.

Assumption 2.11. [8] *For all $i \in \mathbb{S}$ there are matrices $\mathcal{H}_{i1} \geq 0$, $\mathcal{H}_{i2} \geq 0$, and $\mathcal{H}_{i3} \geq 0$ satisfying*

$$\begin{aligned} & \int_{\mathbb{R}} \left[(\hat{\delta}(t) - \hat{A}_i\hat{\delta}_\tau(t) + \mathcal{B}_{2i}\hat{\mu}_i)^T (\hat{\delta}(t) - \hat{A}_i\hat{\delta}_\tau(t) + \mathcal{B}_{2i}\hat{\mu}_i) \right. \\ & \quad \left. - (\hat{\delta}(t) - \hat{A}_i\hat{\delta}_\tau(t))^T (\hat{\delta}(t) - \hat{A}_i\hat{\delta}_\tau(t)) \right] \nu(dy) \\ & \leq \left(\hat{\delta}^T(t)\mathcal{H}_{i1}\hat{\delta}(t) + \hat{\delta}_\tau^T(t)\mathcal{H}_{i2}\hat{\delta}_\tau(t) + \hat{\delta}_\eta^T(t)\mathcal{H}_{i3}\hat{\delta}_\eta(t) \right). \end{aligned}$$

Assumption 2.12. [30] *The function $\hat{\mathbf{f}}(\hat{\delta}(t), \hat{\delta}(t - \eta), \hat{w}(t))$ satisfies*

$$\|\hat{\mathbf{f}}(\hat{\delta}(t), \hat{\delta}(t - \eta), \hat{w}(t))\| \leq \chi\|\hat{\delta}(t)\| + \xi\|\hat{\delta}(t - \eta)\| + \zeta\|\hat{w}(t)\|,$$

where $\chi > 0$, $\xi > 0$, and $\zeta > 0$ are real constants.

3. Design of the controller. This paper presents an approach for designing a control system in which the control input $\hat{u}(t)$, remains constant over specific time intervals and updates only at particular moments. This is achieved through a Zero-Order Hold (ZOH), which ensures that the control signal retains its value throughout each interval. This approach is widely utilized in systems where control actions are executed in discrete time steps. The control signal $\hat{u}(t)$ follows the state feedback law and is described as follows:

$$\hat{u}(t) = K\hat{\delta}(t_p), \quad t_p \leq t < t_{p+1}, \quad (3)$$

where K denotes the feedback gain matrix corresponding to the sampled-data controller that must be determined. $\hat{\delta}(t_p)$ represents the system state sampled in discrete time instants t_p , and the sampling time sequence satisfies:

$$0 = t_0 < t_1 < \dots < t_p < \dots \lim_{p \rightarrow \infty} t_p = +\infty.$$

The sampling instants t_p are assumed to satisfy the condition $t - t_p \leq t_{p+1} - t_p \leq h_p \leq h$ for all $p \geq 0$, where h_p is the variable sampling interval, bounded above by $h > 0$, which represents the maximum sampling period.

4. Formulation of the switching surface. The SMC formulation comprises two main stages. First, a suitable switching surface function $s(t)$ is defined to ensure stable sliding dynamics. Next, a discontinuous SMC law is formulated to move the system trajectories toward the switching surface $s(t) = 0$ within a finite time. To initiate the process, an integral-type switching surface function is chosen for the system.

$$s(t) = \epsilon_i[\hat{\delta}(t) - \hat{A}_i\hat{\delta}_\tau(t)] - \int_0^t \epsilon_i[(\hat{\mathcal{B}}_i + \hat{\mathcal{D}}_i K_i)\hat{\delta}(\theta) + \hat{\mathcal{C}}_i\hat{\delta}(\theta - \eta(\theta))]d\theta, \quad (4)$$

$i \in \mathbb{S}$, $\epsilon_i \in \mathbb{R}^{m \times n}$ meeting $\epsilon_i\hat{\mathcal{D}}_i$ is non singular. The controller gain matrix $K_i \in \mathbb{R}^{m \times n}$ can be determined later.

Remark 4.1. In this paper, the input of the sliding mode controller under consideration is $\hat{\delta}(t_p)$ instead of $\hat{\delta}(t)$.

Applying system (2) and (4), we obtain

$$\dot{s}(t) = \epsilon_i[\Delta\hat{\mathcal{B}}_i\hat{\delta}(t) - \hat{\mathcal{D}}_iK_i\hat{\delta}(t_p) + \Delta\hat{\mathcal{A}}_i\hat{\delta}_\eta(t) + \hat{\mathcal{E}}_i\hat{w}(t)] + \epsilon_i\hat{\mathcal{D}}_i[\hat{u}(t) + \hat{f}(t)]. \quad (5)$$

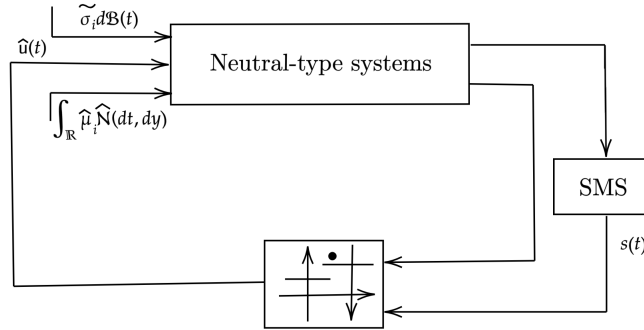
By applying the principles of SMC theory, the trajectories of the closed-loop system move toward the desired switching surface. Hence, when $s(t) = 0$ and $\dot{s}(t) = 0$. Therefore, by $\dot{s}(t) = 0$, and then the equivalent control is given by

$$\hat{u}_{equ}(t) = -(\epsilon_i\hat{\mathcal{D}}_i)^{-1}\epsilon_i(\Delta\hat{\mathcal{B}}_i\hat{\delta}(t) + \Delta\hat{\mathcal{C}}_i\hat{\delta}_\eta(t) + \hat{\mathcal{E}}_i\hat{w}(t)) + K_i\hat{\delta}(t_p) - \hat{f}(t), \quad (6)$$

when incorporating the equivalent control $\hat{u}_{equ}(t)$ for $\hat{u}(t)$ in equation (2), the corresponding sliding mode dynamics or the closed-loop system can be established as

$$\begin{aligned} d[\hat{\delta}(t) - \hat{\mathcal{A}}_i\hat{\delta}_\tau(t)] = & \left\{ [\hat{\mathcal{B}}_i + \Delta\hat{\mathcal{B}}_i - \bar{G}\Delta\hat{\mathcal{B}}_i]\hat{\delta}(t) + \hat{\mathcal{D}}_iK_i\hat{\delta}(t_p) \right. \\ & + [\hat{\mathcal{C}}_i + \Delta\hat{\mathcal{C}}_i - \bar{G}\Delta\hat{\mathcal{C}}_i]\hat{\delta}_\eta(t) + (\hat{\mathcal{E}}_i - \bar{G}\hat{\mathcal{E}}_i)\hat{w}(t) \left. \right\} dt \\ & + \mathcal{B}_{1i}\tilde{\sigma}_i d\mathcal{B}(t) + \mathcal{B}_{2i} \int_{\mathbb{R}} \hat{\mu}_i \hat{\mathcal{N}}(dt, dz), \end{aligned} \quad (7)$$

where $\bar{G} = \hat{\mathcal{D}}_i(\epsilon_i\hat{\mathcal{D}}_i)^{-1}\epsilon_i$.



Sampled-Data Sliding Mode Controller

FIGURE 1. Block diagram of SDSMC for SNTSs

Remark 4.2. The integral switching surface removes the need for the reaching phase that is inherent in the linear switching surface, allowing the system trajectory to start on the sliding surface immediately, and it enhances global robust stability. Consequently, compared to the conventional SMC, the integral SMC is capable of mitigating the drawbacks of chattering.

5. SNTSs analysis via SDSMC. In this study, an SDSMC controller K_i is developed to ensure that system (2) achieves second-moment exponential stability. The stability conditions for nonlinear uncertain stochastic mixed-delay neutral-type systems influenced by Lévy noises are established using a newly constructed discontinuous LKF.

Theorem 5.1. For given scalars $\tau, \eta, h_p, k,$ and c system (7) is assured to be stochastically stable provided that there exist positive definite matrices $P_i, Q, R, S, T, U, \mathcal{V}_i$ any matrices $M_v, X_i, Y_i,$ and positive constants $\hat{\rho}_{\varphi i}$ such that the following LMIs satisfied for $i = 1, 2, v = 1, 2, 3, 4, 5,$ and $\varphi = 1, 2, 3, 4$:

$$\Omega_i = \begin{bmatrix} \bar{\Omega}_{1i} & \bar{\Omega}_{2i} & \bar{\Omega}_{3i} & M_v \\ * & -\alpha I & 0 & 0 \\ * & * & -\alpha I & 0 \\ * & * & * & -\mathcal{V}_1 \end{bmatrix} < 0, \quad (8)$$

$$P_i \leq \hat{\rho}_{1i} I, \quad (9)$$

$$\mathcal{V}_i \leq \hat{\rho}_{2i} I, \quad (10)$$

where

$$\bar{\Omega}_{1i} = \begin{bmatrix} \Omega_{1,1} & \Omega_{1,2} & \Omega_{1,3} & 0 & \Omega_{1,5} & \Omega_{1,6} & \Omega_{1,7} & 0 & \Omega_{1,9} \\ * & \Omega_{2,2} & \Omega_{2,3} & 0 & \Omega_{2,5} & \Omega_{2,6} & 0 & 0 & 0 \\ * & * & \Omega_{3,3} & 0 & \Omega_{3,5} & \Omega_{3,6} & \Omega_{3,7} & 0 & 0 \\ * & * & * & \Omega_{4,4} & 0 & 0 & 0 & 0 & 0 \\ * & * & * & * & \Omega_{5,5} & \Omega_{5,6} & \Omega_{5,7} & 0 & \Omega_{5,9} \\ * & * & * & * & * & \Omega_{6,6} & 0 & 0 & 0 \\ * & * & * & * & * & * & \Omega_{7,7} & 0 & \Omega_{7,9} \\ * & * & * & * & * & * & * & \Omega_{8,8} & 0 \\ * & * & * & * & * & * & * & 0 & \Omega_{9,9} \end{bmatrix},$$

$$\begin{aligned} \Omega_{1,1} &= Q + R + \bar{\eta}S + h_p U + \sum_{j=1}^N \pi_{ij} P_j + \hat{\rho}_{1i} x_{i1} + \hat{\rho}_{3i} \mathcal{H}_{i1} + \hat{\rho}_{2i} x_{i1} \\ &\quad - M_1^T - M_1 + \hat{G}_i^T \hat{G}_i X_i, \quad \Omega_{1,2} = - \sum_{j=1}^N \pi_{ij} P_j \hat{A}_j - M_2^T, \\ \Omega_{1,3} &= M_1 - M_3^T, \quad \Omega_{1,5} = X_i^T \hat{B}_i^T + P_i - M_4^T, \\ \Omega_{1,6} &= M_1 - M_5^T, \quad \Omega_{1,7} = -X_i^T \hat{B}_i^T, \quad \Omega_{1,9} = X_i^T \hat{G}_i^T \hat{H}_i, \quad \Omega_{1,11} = X_i^T \alpha \hat{J}_{ai}^T, \\ \Omega_{2,2} &= -Q + \sum_{j=1}^N \hat{A}_j^T P_j \hat{A}_j + \hat{\rho}_{3i} \mathcal{H}_{i2}, \quad \Omega_{2,3} = M_2, \quad \Omega_{2,5} = -\hat{A}_i P_i, \quad \Omega_{2,6} = M_2, \\ \Omega_{3,3} &= -(1 - \dot{\eta}(t))R + \hat{\rho}_{1i} x_{i2} + \hat{\rho}_{2i} x_{i2} + \hat{\rho}_{3i} \mathcal{H}_{i3} + M_3^T + M_3, \\ \Omega_{3,5} &= X_i^T \hat{C}_i^T + M_4^T, \quad \Omega_{3,6} = M_3 + M_5^T, \quad \Omega_{3,7} = -X_i^T \hat{C}_i^T, \quad \Omega_{3,11} = X_i^T \alpha \hat{J}_{bi}^T, \\ \Omega_{4,4} &= -\frac{(1 - \dot{\eta})}{\eta(t)} S - (1 - \dot{\eta}(t))ck\mathcal{V}_1, \quad \Omega_{5,5} = \bar{\eta}T - X_i^T - X_i, \\ \Omega_{5,6} &= M_4, \quad \Omega_{5,7} = \hat{D}_i Y_i + X_i^T, \quad \Omega_{5,9} = (\hat{E}_i - \bar{G}\hat{E}_i)X_i, \quad \Omega_{5,10} = (\hat{L}_i - \bar{G}\hat{L}_i)X_i, \\ \Omega_{6,6} &= -\frac{(1 - \dot{\eta}(t))}{\eta(t)} T + M_5^T + M_5, \quad \Omega_{7,7} = -\hat{D}_i Y_i, \quad \Omega_{7,9} = -(\hat{E}_i - \bar{G}\hat{E}_i)X_i, \\ \Omega_{7,10} &= (\bar{G}\hat{L}_i - \hat{L}_i)X_i, \quad \Omega_{8,8} = -\frac{U}{h_p^2}, \quad \Omega_{9,9} = -\gamma^2 I + \hat{H}_i^T \hat{H}_i X_i, \end{aligned}$$

and

$$\begin{aligned} \bar{\Omega}_{2i} &= [0 \quad 0 \quad 0 \quad 0 \quad \Omega_{5,10} \quad 0 \quad \Omega_{7,10} \quad 0 \quad 0]^T, \\ \bar{\Omega}_{3i} &= [\Omega_{1,11} \quad 0 \quad \Omega_{3,11} \quad 0 \quad 0 \quad 0 \quad 0 \quad 0 \quad 0]^T, \\ M_v &= [M_1 \quad M_2 \quad M_3 \quad 0 \quad M_4 \quad M_5 \quad 0 \quad 0 \quad 0]^T, \end{aligned}$$

here, the controller gain is computed as $K_i = Y_i X_i^{-1}$ and the remaining elements are zero.

Proof. In order to develop the main results, the LKF is constructed as given below.

$$V(t) = \sum_{i=1}^7 V_i(t), \quad t \in [t_p, t_{p+1}) \quad (11)$$

where

$$\begin{aligned} V_1(t) &= [\hat{\delta}(t) - \hat{A}_i \hat{\delta}_\tau(t)]^T P_i [\hat{\delta}(t) - \hat{A}_i \hat{\delta}_\tau(t)], \\ V_2(t) &= \int_{t-\tau}^t \hat{\delta}^T(s) Q \hat{\delta}(s) ds, \\ V_3(t) &= \int_{t-\eta(t)}^t \hat{\delta}^T(s) R \hat{\delta}(s) ds, \\ V_4(t) &= \int_{-\eta(t)}^0 \int_{t+\theta}^t \hat{\delta}^T(s) S \hat{\delta}(s) ds d\theta, \\ V_5(t) &= \int_{-\eta(t)}^0 \int_{t+\theta}^t g^T(s) T g(s) ds d\theta, \\ V_6(t) &= (t_{p+1} - t) \int_{t_p}^t \hat{\delta}^T(s) U \hat{\delta}(s) ds, \\ V_7(t) &= \int_{-\eta(t)}^0 \int_{t+\theta}^t \text{trace}[\tilde{\sigma}_i^T(s) \mathcal{V}_i \tilde{\sigma}_i(s)] ds d\theta, \end{aligned}$$

and

$$\begin{aligned} g(t) &= \left\{ [\hat{B}_i + \Delta \hat{B}_i - \bar{G} \Delta \hat{B}_i] \hat{\delta}(t) + \hat{D}_i K_i \hat{\delta}(t_p) \right. \\ &\quad \left. + [\hat{C}_i + \Delta \hat{C}_i - \bar{G} \Delta \hat{C}_i] \hat{\delta}_\eta(t) + (\hat{E}_i - \bar{G} \hat{E}_i) \hat{w}(t) \right\}. \end{aligned}$$

By making use of Itô's differential formula [45] and by Lemma 2.6, we can derive the stochastic time derivative of $V_i(t)$ along the paths of systems (2). The resulting expression is given below, where \mathcal{L} denotes the infinitesimal operator of the system.

$$\begin{aligned} \mathcal{L}V_1(t) &= 2\hat{\delta}^T(t) P_i g(t) - 2\hat{A}_i \hat{\delta}_\tau^T P_i g(t) + \text{trace}[\tilde{\sigma}_i^T \mathcal{B}_{1i}^T P_i \mathcal{B}_{1i} \tilde{\sigma}_i] \\ &\quad + \int_{\mathbb{R}} [(\hat{\delta}(t) - \hat{A}_i \hat{\delta}_\tau(t) + \mathcal{B}_{2i} \hat{\mu}_i)^T P_i (\hat{\delta}(t) - \hat{A}_i \hat{\delta}_\tau(t) + \mathcal{B}_{2i} \hat{\mu}_i) \\ &\quad - (\hat{\delta}(t) - \hat{A}_i \hat{\delta}_\tau(t))^T P_i (\hat{\delta}(t) - \hat{A}_i \hat{\delta}_\tau(t))] \nu(dy) \\ &\quad + \sum \pi_{ij} [\hat{\delta}(t) - \hat{A}_i \hat{\delta}_\tau(t)]^T P_j [\hat{\delta}(t) - \hat{A}_i \hat{\delta}_\tau(t)], \end{aligned} \quad (12)$$

$$\mathcal{L}V_2(t) = \hat{\delta}^T(t) Q \hat{\delta}(t) - \hat{\delta}_\tau^T(t) Q \hat{\delta}_\tau(t), \quad (13)$$

$$\mathcal{L}V_3(t) = \hat{\delta}^T(t) R \hat{\delta}(t) - (1 - \hat{\eta}(t)) \hat{\delta}_\eta^T Q \hat{\delta}_\eta(t), \quad (14)$$

$$\mathcal{L}V_4(t) = \bar{\eta} \hat{\delta}^T(t) S \hat{\delta}(t) - (1 - \hat{\eta}(t)) \int_{t-\eta(t)}^t \hat{\delta}(s)^T S \hat{\delta}(s) ds, \quad (15)$$

$$\mathcal{L}V_5(t) = \bar{\eta} g^T(t) T g(t) - (1 - \hat{\eta}(t)) \int_{t-\eta(t)}^t g^T(s) T g(s) ds, \quad (16)$$

$$\mathcal{L}V_6(t) = h_p \hat{\delta}^T(t) U \hat{\delta}(t) - \int_{t_p}^t \hat{\delta}^T(s) U \hat{\delta}(s) ds, \quad (17)$$

$$\mathcal{L}V_7(t) = \bar{\eta} \text{trace}[\tilde{\sigma}_i^T \mathcal{B}_{2i}^T \mathcal{V}_i \tilde{\sigma}_i \mathcal{B}_{2i}]$$

$$- (1 - \hat{\eta}(t)) \int_{t-\eta(t)}^t \text{trace}[\tilde{\sigma}_i^T(s) \mathcal{B}_{2i}^T \mathcal{V}_i \tilde{\sigma}_i(s) \mathcal{B}_{2i}(s)] ds. \quad (18)$$

Based on Assumptions 2.10 and 2.11, the following results are obtained:

$$\text{trace}[\tilde{\sigma}_i^T \mathcal{B}_{1i}^T P_i \mathcal{B}_{1i} \tilde{\sigma}_i] \leq \hat{\rho}_{1i} \left(\hat{\delta}^T(t) x_{i1} \hat{\delta}(t) + \hat{\delta}_\eta^T(t) x_{i2} \hat{\delta}_\eta \right),$$

$$\text{trace}[\tilde{\sigma}_i^T \mathcal{B}_{2i}^T \mathcal{V}_i \mathcal{B}_{2i} \tilde{\sigma}_i] \leq \hat{\rho}_{2i} \left(\hat{\delta}^T(t) x_{i1} \hat{\delta}(t) + \hat{\delta}_\eta^T(t) x_{i2} \hat{\delta}_\eta \right),$$

and

$$\begin{aligned} & \int_{\mathbb{R}} [(\hat{\delta}(t) - \hat{A}_i \hat{\delta}_\tau(t) + \mathcal{B}_{2i} \mu_i)^T P_i (\hat{\delta}(t) - \hat{A}_i \hat{\delta}_\tau(t) + \mathcal{B}_{2i} \mu_i) \\ & \quad - (\hat{\delta}(t) - \hat{A}_i \hat{\delta}_\tau(t))^T P_i (\hat{\delta}(t) - \hat{A}_i \hat{\delta}_\tau(t))] \nu(dy) \\ & \leq \hat{\rho}_{3i} \left(\hat{\delta}^T(t) \mathcal{H}_{i1} \hat{\delta}(t) + \hat{\delta}_\tau^T(t) \mathcal{H}_{i2} \hat{\delta}_\tau(t) + \hat{\delta}_\eta^T(t) \mathcal{H}_{i3} \hat{\delta}_\eta(t) \right), \end{aligned}$$

the following result can be directly derived by

$$\begin{aligned} & \sum_{j=1}^N \pi_{ij} [\hat{\delta}(t) - \hat{A}_i \hat{\delta}_\tau(t)]^T P_j [\hat{\delta}(t) - \hat{A}_i \hat{\delta}_\tau(t)] \\ & = \sum_{j=1}^N \pi_{ij} [\hat{\delta}^T(t) P_j \hat{\delta}(t) - \hat{\delta}^T(t) P_j \hat{A}_j \hat{\delta}_\tau(t) \\ & \quad - \hat{\delta}_\tau^T(t) \hat{A}_j^T P_j \hat{\delta}(t) + \hat{\delta}_\tau^T(t) \hat{A}_j^T P_j \hat{\delta}_\tau(t)]. \end{aligned}$$

Lemma 2.3 enables the integral components in (15)–(18) to be represented as follows.

$$- \int_{t-\eta(t)}^t \hat{\delta}^T(t) S \hat{\delta}(t) ds \leq - \frac{1}{\eta(t)} \left(\int_{t-\eta(t)}^t \hat{\delta}(s) ds \right)^T S \left(\int_{t-\eta(t)}^t \hat{\delta}(s) ds \right), \quad (19)$$

$$- \int_{t-\eta(t)}^t g^T(s) T g(s) ds \leq - \frac{1}{\eta(t)} \left(\int_{t-\eta(t)}^t g(s) ds \right)^T T \left(\int_{t-\eta(t)}^t g(s) ds \right), \quad (20)$$

$$- \int_{t_p}^t \hat{\delta}^T(s) U \hat{\delta}(s) ds \leq - \frac{1}{h_p^2} \left(\int_{t_p}^t \hat{\delta}(s) ds \right)^T U \left(\int_{t_p}^t \hat{\delta}(s) ds \right). \quad (21)$$

Using the Newton–Leibniz formula, a zero equation can be formulated for any admissible matrices M_v and N ,

$$2\beta^T(t) M_v \left[\hat{\delta}_\eta - \hat{\delta}(t) + \int_{t-\eta}^t g(s) ds + \int_{t-\eta}^t \tilde{\sigma}_i(s) d\mathcal{B}(s) + \bar{\mu}_i \right] = 0,$$

where $\beta^T(t) = [\hat{\delta}^T(t) \hat{\delta}_\tau^T \hat{\delta}_\eta^T \int_{t-\eta}^t \hat{\delta}^T(s) ds \ g^T(t) \int_{t-\eta}^t g^T(s) ds \ \hat{\delta}^T(t_p) \int_{t_p}^t \hat{\delta}^T(s) ds \ w^T(t)]$ and $\bar{\mu}_i = \int_{t-\eta}^t \int_{\mathbb{R}} \hat{\mu}_i \hat{N}(dt, dy)$.

The stochastic term in the above inequality can be rewritten by applying Lemma 2.4:

$$\begin{aligned} & 2\beta^T(t) M_v \int_{t-\eta}^t \tilde{\sigma}_i(s) d\mathcal{B}(s) \leq \beta^T(t) M_v \mathcal{V}_1^{-1} M_v^T \beta(t) \\ & \quad + \left(\int_{t-\eta}^t \tilde{\sigma}_i(s) d\mathcal{B}(s) \right)^T \mathcal{V}_1 \left(\int_{t-\eta}^t \tilde{\sigma}_i(s) d\mathcal{B}(s) \right), \end{aligned} \quad (22)$$

$$2\beta^T(t)M_v\bar{\mu}_i \leq \beta^T(t)M_v\mathcal{V}_2^{-1}M_v^T\beta(t) + \bar{\mu}_i^T\mathcal{V}_2\bar{\mu}_i, \quad (23)$$

the other zero equation is considered as

$$2[g^T - \hat{\delta}^T(t_p)]N \left[\left\{ [\hat{\mathcal{B}}_i + \Delta\hat{\mathcal{B}}_i - \bar{G}\Delta\hat{\mathcal{B}}_i]\hat{\delta}(t) + \hat{\mathcal{D}}_iK_i\hat{\delta}(t_p) \right. \right. \\ \left. \left. + [\hat{\mathcal{C}}_i + \Delta\hat{\mathcal{C}}_i - \bar{G}\Delta\hat{\mathcal{C}}_i]\hat{\delta}_\eta(t) + (\hat{\mathcal{E}}_i - \bar{G}\hat{\mathcal{E}}_i)\hat{w}(t) \right\} - g(t) \right] = 0. \quad (24)$$

Now, taking expectation for stochastic terms appeared in (22) and (23), using Assumption 2.9, we get

$$\begin{aligned} \bar{\mu}_i^T\mathcal{V}_2\bar{\mu}_i &\leq \rho_{4i}c\mathbb{E} \left[\left(\int_{t-\eta}^t \int_{\mathbb{R}} (\bar{\mu}(\hat{\delta}(s-), y))^2 \nu(dy) ds \right) \right] \\ &\leq \rho_{4i}c\mathbb{E} \left[\left(\int_{t-\eta}^t \left(\int_{\mathbb{R}} \bar{\mu}(\hat{\delta}(s-), y)^2 \nu(dy) \right) ds \right) \right] \\ &\leq \rho_{4i}ck\mathbb{E} \left[\left(\int_{t-\eta}^t \hat{\delta}^2(s) ds \right) \right]. \end{aligned} \quad (25)$$

As established in Øksendal [22], the following inequality holds:

$$\mathbb{E} \left[\int_{t-\eta}^t \tilde{\sigma}_i^T d\mathcal{B}(s) \mathcal{V}_1 \int_{t-\eta}^t \tilde{\sigma}_i d\mathcal{B}(s) \right] \leq \mathbb{E} \left[\int_{t-\eta}^t \text{trace}(\tilde{\sigma}_i^T(s) \mathcal{V}_1 \tilde{\sigma}_i(s)) ds \right].$$

Combining (12)-(25), we get

$$\begin{aligned} \mathbb{E}[\mathcal{L}V(t)] &\leq 2\hat{\delta}^T(t)P_i g(t) + 2\hat{\mathcal{A}}_i \hat{\delta}^T(t)P_i g(t) \\ &\quad + \hat{\rho}_{1i}(\hat{\delta}^T(t)x_{i1}\hat{\delta}(t)) + \hat{\rho}_{1i}(\hat{\delta}_\eta^T(t)x_{i2}\hat{\delta}_\eta(t)) \\ &\quad + \hat{\rho}_{3i}(\hat{\delta}^T(t)\mathcal{H}_{i1}\hat{\delta}(t)) + \hat{\rho}_{3i}(\hat{\delta}_\tau^T(t)\mathcal{H}_{i2}\hat{\delta}_\tau(t)) + \hat{\rho}_{3i}(\hat{\delta}_\eta^T(t)\mathcal{H}_{i3}\hat{\delta}_\eta(t)) \\ &\quad + \sum_{j=1}^N \pi_{ij}\hat{\delta}^T(t)P_j\hat{\delta}(t) - \sum_{j=1}^N \pi_{ij}\hat{\delta}^T(t)P_j\hat{\mathcal{A}}_j\hat{\delta}_\tau(t) \\ &\quad - \sum_{j=1}^N \pi_{ij}\hat{\delta}_\tau^T(t)\hat{\mathcal{A}}_j^T P_j\hat{\delta}(t) + \sum_{j=1}^N \pi_{ij}\hat{\delta}_\tau^T(t)\hat{\mathcal{A}}_j^T P_j\hat{\mathcal{A}}_j\hat{\delta}_\tau(t) \\ &\quad + \hat{\delta}^T(t)Q\hat{\delta}(t) - \hat{\delta}_\tau^T(t)Q\hat{\delta}_\tau(t) + \hat{\delta}^T(t)R\hat{\delta}(t) - (1 - \eta(t))\hat{\delta}_\eta^T(t)R\hat{\delta}_\eta(t) \\ &\quad + \bar{\eta}\hat{\delta}^T(t)S\hat{\delta}(t) - \frac{(1 - \eta(t))}{\eta(t)} \left(\int_{t-\eta(t)}^t \hat{\delta}(s) ds \right)^T S \left(\int_{t-\eta(t)}^t \hat{\delta}(s) ds \right) \\ &\quad + \bar{\eta}g^T(t)Tg(t) - \frac{(1 - \eta(t))}{\eta(t)} \left(\int_{t-\eta(t)}^t g(s) ds \right)^T T \left(\int_{t-\eta(t)}^t g(s) ds \right) \\ &\quad + h_p\hat{\delta}^T(t)U\hat{\delta}(t) - \frac{1}{h_p^2} \left(\int_{t_p}^t \hat{\delta}(s) ds \right)^T U \left(\int_{t_p}^t \hat{\delta}(s) ds \right) \\ &\quad + \hat{\rho}_{2i}(\hat{\delta}^T(t)x_{i1}\hat{\delta}(t)) + \hat{\rho}_{2i}(\hat{\delta}_\eta^T(t)x_{i2}\hat{\delta}_\eta(t)) - (1 - \eta(t))ck\mathcal{V}_1 \\ &\quad + 2g^T(t)N\hat{\mathcal{B}}_i\hat{\delta}(t) + 2g^T N\Delta\hat{\mathcal{B}}_i\hat{\delta}(t) - 2g^T(t)N\bar{G}\Delta\hat{\mathcal{B}}_i\hat{\delta}(t) \\ &\quad + 2g^T N\hat{\mathcal{D}}_iK_i\hat{\delta}(t) + 2g^T(t)N\hat{\mathcal{C}}_i\hat{\delta}_\eta(t) + 2g^T(t)N\Delta\hat{\mathcal{C}}_i\hat{\delta}_\eta(t) \\ &\quad + 2g^T(t)N(\hat{\mathcal{E}}_i - \bar{G}\hat{\mathcal{E}}_i) - 2g^T(t)N\bar{G}\Delta\hat{\mathcal{C}}_i\hat{\delta}_\eta(t) - 2g^T(t)Ng(t) \\ &\quad - 2\hat{\delta}^T(t_p)N\hat{\mathcal{B}}_i\hat{\delta}(t)\hat{w}(t) - 2\hat{\delta}^T(t_p)N\Delta\hat{\mathcal{B}}_i\hat{\delta}(t) + 2\hat{\delta}^T(t_p)N\bar{G}\Delta\hat{\mathcal{B}}_i\hat{\delta}(t) \end{aligned}$$

$$\begin{aligned}
& -2\delta^T(t_p)N\hat{D}_iK_i\delta(t_p) - \hat{\delta}^T(t_p)N\hat{C}_i\hat{\delta}_\eta(t) - 2\hat{\delta}^T(t_p)N\Delta\hat{C}_i\hat{\delta}_\eta(t) \\
& + 2\hat{\delta}^T(t_p)N\bar{G}\Delta\hat{C}_i\delta_\eta(t) + 2g^T(t_p)Ng(t) - 2g^T(t)N(\hat{E}_i - \bar{G}\hat{E}_i), \\
& \leq \mathbb{E}[\beta^T(t)\Psi\beta(t)], \tag{26}
\end{aligned}$$

where $\Psi = \Omega + M_1\mathcal{V}_1^{-1}M_1^T + M_2\mathcal{V}_1^{-1}M_2^T + M_3\mathcal{V}_1^{-1}M_3^T + M_4\mathcal{V}_1^{-1}M_4^T + M_5\mathcal{V}_1^{-1}M_5^T$. Let $X_i = (N^{-1})^T$, $K_i = Y_iX_i^{-1}$. For the uncertainty terms appearing in (26), by employing Lemma 2.2, together with pre- and post-multiplication of (26) by $\text{diag}\{N^{-1}, N^{-1}, N^{-1}, N^{-1}, N^{-1}, N^{-1}, N^{-1}, N^{-1}, I, I, I, I\}$ and by Lemma 2.5, the LMIs (8)–(10) can be obtained. Hence, since $\Psi < 0$, it follows that $\mathbb{E}[\mathcal{L}V(t)] \leq 0$, indicating that the considered system is stochastically stable.

In addition, we analyze the performance H_∞ of the system (1) along with its controlled output by defining a performance index H_∞ to evaluate the attenuation capacity of the disturbance $\gamma > 0$.

$$J = \left[\int_0^\infty [\dot{\mathbf{z}}^T(t)\dot{\mathbf{z}}(t) - \gamma^2\dot{\mathbf{w}}^T(t)\dot{\mathbf{w}}(t)] dt \right], \tag{27}$$

where

$$\dot{\mathbf{z}}(t) = \hat{G}_i\hat{\delta}(t) + \hat{H}_i\hat{w}(t).$$

According to Definition 2.8 and the given initial conditions, it follows that $V(0) = 0$ and $V(\infty) \geq 0$. Therefore,

$$\begin{aligned}
J & \leq \mathbb{E} \int_0^\infty [\dot{\mathbf{z}}^T(t)\dot{\mathbf{z}}(t) - \gamma^2\dot{\mathbf{w}}^T(t)\dot{\mathbf{w}}(t)] dt + V\hat{\delta}(t)|_{t \rightarrow \infty} - V\hat{\delta}(t)|_{t=0} \\
& \leq \mathbb{E} \int_0^\infty [\dot{\mathbf{z}}^T(t)\dot{\mathbf{z}}(t) - \gamma^2\dot{\mathbf{w}}^T(t)\dot{\mathbf{w}}(t)] dt + \mathcal{L}V\hat{\delta}(t) \\
& \leq \mathbb{E} \left[\int_0^\infty \beta_1^T(t)\Omega_w\beta_1(t) \right],
\end{aligned}$$

where

$$\Omega_w = \begin{bmatrix} [\Omega]_{8 \times 8} & \Omega_{1,9} \\ * & \Omega_{9,9} \end{bmatrix}, \tag{28}$$

$[\Omega]_{8 \times 8} = \Omega_{1,1} + \hat{G}_i^T\hat{G}_i$, $\Omega_{1,9} = \hat{G}_i^T\hat{H}_i$, $\Omega_{9,9} = -\gamma^2I + \hat{H}_i^T\hat{H}_i$, and $\beta_1(t) = [\beta^T(t) \dot{\mathbf{w}}^T(t)]$.

Thus, it follows that the performance index $J \leq 0$ holds, whenever $\Omega_w < 0$, which can be easily verified as

$$\mathbb{E}[\|\dot{\mathbf{z}}(t)\|_2 \leq \|\dot{\mathbf{w}}(t)\|_2].$$

This indicates that $\Omega_i < 0$. Consequently, the examined system is stochastically stable at a disturbance attenuation level of $\gamma > 0$. As a result, it can be concluded that $\mathcal{L}V(t) < 0$. According to (26), one obtains

$$\mathcal{L}V \leq -\Lambda_i\|\hat{\delta}(t)\|^2 \leq -\hat{\Lambda}\|\hat{\delta}(t)\|^2, \tag{29}$$

where $-\Lambda_i = \lambda_{\max}(\Omega_i)$ ($\Lambda_i > 0$), $-\hat{\Lambda} = \max_{i \in \mathbb{S}}\{-\Lambda_i\}$, $\lambda_{\max}(\Omega_i)$ represents the maximum eigenvalue of Ω_i .

Based on Dynkin's formula [44], we obtain the following result:

$$-\mathbb{E} \int_0^T \mathcal{L}V dt = \mathbb{E}V_0 - \mathbb{E}V_T \leq \mathbb{E}V_0. \tag{30}$$

From (29)–(30), we get

$$\mathbb{E} \int_0^T \|\hat{\delta}(t)\|^2 dt \leq \frac{1}{\Lambda} \mathbb{E}V_0 < \infty.$$

Based on Definition 2.7, system (7) is verified to be second-moment exponentially stable. Therefore, the proof is concluded. \square

Remark 5.2. It is worth noting that the Lyapunov functional in (11) incorporates the term $V_6(t)$, which explicitly depend on the sampling interval (t_p, t_{p+1}) . This term allow the functional to fully exploit information related to the actual sampling behavior. As a result, the derived synchronization condition is less conservative.

6. Reachability analysis of the switching surface. An SDSMC law is developed in this section, using the switching surface (4), to ensure that the system trajectory approaches the switching surface. The reachability of the trajectory is ensured by the following theorem.

Theorem 6.1. *If the feasibility of LMIs (8), (9), and (10) is ensured, then the state trajectories of the system (7) will be driven to the switching surface (4) by applying the SDSMC law is designed as follows.*

$$\hat{u}(t) = \hat{u}_1 - \hat{u}_2 - \hat{u}_3, \quad (31)$$

with

$$\begin{aligned} \hat{u}_1 &= K_i \hat{\delta}(t_p), \\ \hat{u}_2 &= (\chi(t) \|\hat{\delta}(t)\| + \xi(t) \|\hat{\delta}_\eta(t)\| + \zeta(t) \|\hat{w}(t)\|) \text{sgn}(s^T(t) \epsilon_i \hat{D}_i)^T, \\ \hat{u}_3 &= \frac{\varepsilon + \|\epsilon_i\| \|\hat{L}_i\| (\|\hat{J}_a\| \|\hat{\delta}(t)\| + \|\hat{J}_b\| \|\hat{\delta}_\eta(t)\|)}{\|\epsilon_i \hat{D}_i\|} \text{sgn}(s^T(t) \epsilon_i \hat{D}_i)^T, \end{aligned}$$

here, $\varepsilon > 0$, $\chi(t)$, $\xi(t)$, and $\zeta(t)$ are used to evaluate $\bar{\chi}$, $\bar{\xi}$, and $\bar{\zeta}$, respectively. These are defined as follows:

$$\begin{aligned} \tilde{\chi}(t) &= \chi(t) - \phi, \quad \dot{\tilde{\chi}}(t) = \|s^T(t)\| \|\epsilon_i \hat{D}_i\| \|\hat{\delta}(t)\|, \\ \tilde{\xi}(t) &= \xi(t) - \xi, \quad \dot{\tilde{\xi}}(t) = \|s^T(t)\| \|\epsilon_i \hat{D}_i\| \|\hat{\delta}_\eta(t)\|, \\ \tilde{\zeta}(t) &= \zeta(t) - \zeta, \quad \dot{\tilde{\zeta}}(t) = \|s^T(t)\| \|\epsilon_i \hat{D}_i\| \|\hat{w}(t)\|, \end{aligned} \quad (32)$$

where $\tilde{\chi}(t)$, $\tilde{\xi}(t)$, and $\tilde{\zeta}(t)$ denote the estimation errors.

Proof. Consider the Lyapunov function designed as follows:

$$V(t) = \frac{1}{2} (s^T(t) s(t) + \tilde{\chi}^2(t) + \tilde{\xi}^2(t) + \tilde{\zeta}^2(t)). \quad (33)$$

Based on equations (5), (31), (32), and the Itô derivative corresponding to the Lyapunov function in (33) is given by

$$\begin{aligned} \mathcal{L}V(t) &= s^T(t) \dot{s}(t) + \tilde{\chi}(t) \dot{\tilde{\chi}}(t) + \tilde{\psi}(t) + \dot{\tilde{\psi}}(t) + \tilde{\zeta}(t) \dot{\tilde{\zeta}}(t) \\ &= s^T(t) (\epsilon_i [\Delta \hat{B}_i \hat{\delta}(t) - \hat{D}_i K_i \hat{\delta}(t_p) + \Delta \hat{A}_i \hat{\delta}_\eta(t) + \hat{E} \hat{w}(t)] \\ &\quad + \epsilon_i \hat{D}_i [\hat{u}(t) + \hat{f}(t)]) + \tilde{\chi}(t) \dot{\tilde{\chi}}(t) + \tilde{\xi}(t) \dot{\tilde{\xi}}(t) + \tilde{\zeta}(t) \dot{\tilde{\zeta}}(t) \\ &\leq \|s^T(t)\| \|\epsilon_i\| \|\hat{L}_i\| \|\hat{J}_a\| \|\hat{\delta}(t)\| + \|s^T(t)\| \|\epsilon_i\| \|\hat{L}\| \|\hat{J}_b\| \|\hat{\delta}_\eta(t)\| \\ &\quad - s^T(t) \epsilon_i \hat{D}_i \hat{u}_2(t) - s^T(t) \epsilon_i \hat{D}_i \hat{u}_3(t) + s^T(t) \epsilon_i \hat{D}_i \hat{w}(t) \end{aligned} \quad (34)$$

$$\begin{aligned}
& + s^T(t)\epsilon_i\hat{D}_if(t) + \tilde{\chi}(t)\|s^T(t)\| \|\epsilon_i\hat{D}_i\| \|\hat{\delta}(t)\| \\
& + \tilde{\xi}(t)\|s^T(t)\| \|\epsilon_i\hat{D}_i\| \|\hat{\delta}_\eta(t)\| + \tilde{\zeta}(t)\|s^T(t)\| \|\epsilon_i\hat{D}_i\| \|\hat{w}(t)\|.
\end{aligned}$$

From Assumption 2.12 and (32), we get

$$\begin{aligned}
& - s^T(t)\epsilon_i\hat{D}_i\hat{u}_2(t) + s^T(t)\epsilon_i\hat{D}_if(t) + s^T(t)\epsilon_i\hat{D}_i\hat{w}(t) \\
& + \tilde{\chi}(t)\|s^T(t)\| \|\epsilon_i\hat{D}_i\| \|\hat{\delta}(t)\| + \tilde{\xi}(t)\|s^T(t)\| \|\epsilon_i\hat{D}_i\| \|\hat{\delta}_\eta(t)\| \\
& + \tilde{\zeta}(t)\|s^T(t)\| \|\epsilon_i\hat{D}_i\| \|\hat{w}(t)\| \\
& \leq -\|s^T(t)\epsilon_i\hat{D}_i\|(\chi(t)\|\hat{\delta}(t)\| + \xi(t)\|\hat{\delta}_\eta(t)\| + \zeta(t)\|\hat{w}(t)\|) \\
& + \tilde{\chi}(t)\|s^T(t)\| \|\epsilon_i\hat{D}_i\| \|\hat{\delta}(t)\| + \tilde{\xi}(t)\|s^T(t)\| \|\epsilon_i\hat{D}_i\| \|\hat{\delta}_\eta(t)\| \\
& + \tilde{\zeta}(t)\|s^T(t)\| \|\epsilon_i\hat{D}_i\| \|\hat{w}(t)\| + s^T(t)\epsilon_i\hat{D}_if(t) + s^T(t)\epsilon_i\hat{D}_i\hat{w}(t) \\
& = -\tilde{\chi}(t)\|s^T(t)\| \|\epsilon_i\hat{D}_i\| \|\hat{\delta}(t)\| - \tilde{\xi}(t)\|s^T(t)\| \|\epsilon_i\hat{D}_i\| \|\hat{\delta}_\eta(t)\| \\
& - \tilde{\zeta}(t)\|s^T(t)\| \|\epsilon_i\hat{D}_i\| \|\hat{w}(t)\| + s^T(t)\epsilon_i\hat{D}_if(t) + s^T(t)\epsilon_i\hat{D}_i\hat{w}(t) \\
& \leq 0.
\end{aligned} \tag{35}$$

Based on (31), (34), and (35), we get

$$\begin{aligned}
\mathcal{LV}(t) & \leq \|s^T(t)\| \|\epsilon_i\| \|\hat{L}_i\| \|\hat{J}_{ai}\| \|\hat{\delta}(t)\| + \|s^T(t)\| \|\epsilon_i\| \|\hat{L}_i\| \|\hat{J}_{bi}\| \|\hat{\delta}_\eta(t)\| \\
& - s^T\epsilon_i\hat{D}_i\hat{u}_3(t) \\
& \leq \|s^T(t)\| \|\epsilon_i\| \|\hat{L}_i\| \|\hat{J}_{ai}\| \|\hat{\delta}(t)\| + \|s^T(t)\| \|\epsilon_i\| \|\hat{L}_i\| \|\hat{J}_{bi}\| \|\hat{\delta}_\eta(t)\| \\
& - \|s^T(t)\epsilon_i\hat{D}_i\| \frac{\varepsilon + \|\epsilon_i\| \|\hat{L}_i\| (\|\hat{J}_{ai}\| \|\hat{\delta}(t)\| + \|\hat{J}_{bi}\| \|\hat{\delta}_\eta(t)\|)}{\|\epsilon_i\hat{D}_i\|}, \\
& \leq -\varepsilon\|s(t)\| < 0, \quad \text{for } \|s(t)\| \neq 0
\end{aligned} \tag{36}$$

where $\varepsilon > 0$.

From (32), we have $\dot{\chi}(t) = \dot{\tilde{\chi}}(t) = \|s^T(t)\| \|\epsilon_i\hat{D}_i\| \|\hat{\delta}(t)\| \geq 0$, $\dot{\xi}(t) = \dot{\tilde{\xi}}(t) = \|s^T(t)\| \|\epsilon_i\hat{D}_i\| \|\hat{\delta}_\eta(t)\| \geq 0$, and $\dot{\zeta}(t) = \dot{\tilde{\zeta}}(t) = \|s^T(t)\| \|\epsilon_i\hat{D}_i\| \|\hat{w}(t)\| \geq 0$. Thus, $\tilde{\chi}(t)$, $\tilde{\xi}(t)$ and $\tilde{\zeta}(t)$ are monotonically non-decreasing. Consequently, there exists a time instant $t^* > 0$ such that

$$\tilde{\chi}(t) = \chi(t) - \bar{\chi} \geq 0, \quad \tilde{\xi}(t) = \xi(t) - \bar{\xi} \geq 0, \quad \tilde{\zeta}(t) = \zeta(t) - \bar{\zeta} \geq 0.$$

Clearly, $\tilde{\chi}(t)\dot{\tilde{\chi}}(t) \geq 0$, $\tilde{\xi}(t)\dot{\tilde{\xi}}(t) \geq 0$, and $\tilde{\zeta}(t)\dot{\tilde{\zeta}}(t) \geq 0$. From (36), it follows that $s^T(t)\dot{s}(t) < 0$. Hence, the reaching condition given in (4) is fulfilled, which ensures that the trajectories of the sliding mode dynamics (7) converge to the switching surface within a finite time. This concludes the proof. \square

Remark 6.2. The proof of the theorem is nontrivial and makes use of advanced techniques, including Lévy-type stochastic integrals and the Lévy–Itô formula. These methods are significantly more complex than those typically applied to classical stochastic differential equations driven by Brownian motion.

Remark 6.3. The obtained sufficient conditions are expressed in terms of LMI's, utilizing the zero equation to alleviate potential conservatism. However, it is widely acknowledged that introducing zero equations considerably enlarges the set of decision variables, thereby complicating the conditions, increasing computational effort, and extending the solution time.

Remark 6.4. The parameter ε is an important component of the adaptive control law, since it has a direct influence on the convergence behavior of the sliding surface. If ε is chosen too large, the resulting control action may become excessively strong and impractical for real applications. In contrast, when ε is too small, the sliding variable may remain outside the boundary layer, which can increase adaptive gains and induce oscillatory behavior on the sliding manifold. Therefore, the value of ε should be selected with care to achieve a suitable compromise between convergence speed and control performance.

Remark 6.5. The adaptive sliding mode control law is composed of multiple terms, each serving a distinct purpose. The term \hat{u}_1 is designed to counteract known system dynamics, while \hat{u}_2 is introduced to compensate for unknown nonlinearities through adaptive estimation. The remaining component \hat{u}_3 addresses parametric uncertainties and includes a boundary parameter that guarantees the reachability of the sliding surface. Together, these components ensure robustness and stable sliding motion of the closed-loop system.

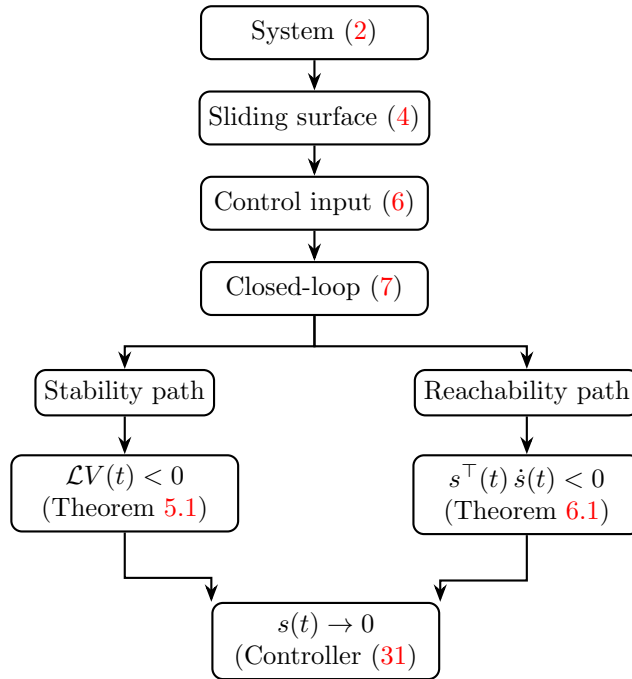


FIGURE 2. Workflow of the proposed controller

As shown in Figure 1 the SDSMC for SNTSs is represented by its block diagram. Complementing this, Figure 2 displays the algorithm workflow that summarizes the key steps leading to the main results.

7. Numerical examples. Two illustrative examples are provided in this section to demonstrate the efficiency of the designed SDSMC based on the Lévy-type noise technique.

Example 1. A two-dimensional SNTSs (2) featuring two Markovian switching modes is analyzed, with the corresponding parameters specified as follows:

$$\begin{aligned}\hat{\mathcal{A}}_1 &= \begin{bmatrix} 2 & 0.8 \\ 0 & 3 \end{bmatrix}, \hat{\mathcal{A}}_2 = \begin{bmatrix} 0.4 & -0.4 \\ 0 & 4 \end{bmatrix}, \hat{\mathcal{B}}_1 = \hat{\mathcal{B}}_2 = \begin{bmatrix} 1 & 0 \\ 0 & 1 \end{bmatrix}, \hat{\mathcal{C}}_1 = \begin{bmatrix} 0.7 & 0.7 \\ 0.8 & 0.8 \end{bmatrix}, \\ \hat{\mathcal{C}}_2 &= \begin{bmatrix} 0.2 & 0.7 \\ 0.02 & 0.8 \end{bmatrix}, \hat{\mathcal{D}}_1 = \begin{bmatrix} 2.5 & 0.0025 \\ 0.005 & 0.5 \end{bmatrix}, \hat{\mathcal{D}}_2 = \begin{bmatrix} 0.55 & -5 \\ 0.5 & 5 \end{bmatrix}, \\ \hat{\mathcal{E}}_1 &= \begin{bmatrix} 0.25 & 0.25 \\ 0.5 & 0.5 \end{bmatrix}, \hat{\mathcal{E}}_2 = \begin{bmatrix} 2 & 2.5 \\ 0.05 & 0.5 \end{bmatrix}, \hat{\mathcal{G}}_1 = \begin{bmatrix} 0.002 & 0.002 \\ 0.004 & 0.004 \end{bmatrix}, \\ \hat{\mathcal{G}}_2 &= \begin{bmatrix} 2 & 2.5 \\ 0.05 & 0.5 \end{bmatrix}, \hat{\mathcal{H}}_1 = \begin{bmatrix} 0.001 & 0 \\ 0 & 0.003 \end{bmatrix}, \hat{\mathcal{H}}_2 = \begin{bmatrix} 0.1 & 0.1 \\ 0.2 & 0.03 \end{bmatrix},\end{aligned}$$

when addressing the uncertainty terms, we present the matrix that incorporates the uncertainties, as shown below.

$$\begin{aligned}\hat{\mathcal{J}}_{a1} &= \begin{bmatrix} -0.002 & -0.004 \\ 0 & 0 \end{bmatrix}, \hat{\mathcal{J}}_{a2} = \begin{bmatrix} -2 & 4 \\ -0.1 & 0.08 \end{bmatrix}, \hat{\mathcal{J}}_{b1} = \begin{bmatrix} -0.002 & -0.004 \\ 0 & 0 \end{bmatrix}, \\ \hat{\mathcal{J}}_{b2} &= \begin{bmatrix} -0.002 & 0.04 \\ 0.1 & 0.1 \end{bmatrix}, \hat{\mathcal{L}}_1 = \hat{\mathcal{L}}_2 = \begin{bmatrix} 1 & 0 \\ 0 & 2 \end{bmatrix}, \\ x_{11} = x_{12} = x_{21} &= \begin{bmatrix} 0.1 & 0 \\ 0 & 0.1 \end{bmatrix}, x_{22} = \begin{bmatrix} 2 & 0 \\ 7 & 0.1 \end{bmatrix},\end{aligned}$$

where x_{1i} and x_{2i} are the terms that arise in solving the trace terms.

$$\begin{aligned}\mathcal{H}_{11} &= \begin{bmatrix} 1 & 0 \\ 0 & 0.4 \end{bmatrix}, \mathcal{H}_{21} = \begin{bmatrix} 0.4 & 0 \\ 0 & 0.4 \end{bmatrix}, \mathcal{H}_{12} = \begin{bmatrix} 2 & 0 \\ 0 & 0.35 \end{bmatrix}, \\ \mathcal{H}_{13} &= \begin{bmatrix} 0.003 & 0 \\ 0 & 0.3 \end{bmatrix}, \mathcal{H}_{22} = \begin{bmatrix} -0.5 & 0 \\ 0 & 3.5 \end{bmatrix}, \mathcal{H}_{23} = \begin{bmatrix} 3 & 0 \\ 5 & 0.3 \end{bmatrix},\end{aligned}$$

the system time delay is taken to be $\tau = 0.6$, $\eta = 0.5$, and $\dot{\eta} = 0.4$. The constants are $c = 0.2$, and $k = \begin{bmatrix} 2 & 5 \\ 0.1 & 1.05 \end{bmatrix}$. Also, $h_p = 0.4$, $\pi = 0.3$, $\alpha = 0.1$, and $\gamma = 0.9$.

Then, solving the LMI using MATLAB, we can get

$$\begin{aligned}P_1 &= \begin{bmatrix} 0.0251 & -0.0084 \\ -0.0084 & 0.0311 \end{bmatrix}, P_2 = \begin{bmatrix} 0.1050 & 0.0001 \\ 0.0001 & 0.0605 \end{bmatrix}, \\ Q &= \begin{bmatrix} 1.0085 & -0.0659 \\ -0.0659 & 1.5469 \end{bmatrix}, R = \begin{bmatrix} 3.3634 & 2.5401 \\ 2.5401 & 2.8703 \end{bmatrix}, \\ S &= \begin{bmatrix} 1.0355 & -0.5831 \\ -0.5831 & 1.0195 \end{bmatrix}, T = \begin{bmatrix} 0.5327 & 0.0843 \\ 0.0843 & 0.3965 \end{bmatrix}, \\ U &= \begin{bmatrix} 0.4581 & -0.0083 \\ -0.0083 & 0.4669 \end{bmatrix}, \mathcal{V}_1 = \begin{bmatrix} 7.3592 & 2.2499 \\ 2.2499 & 7.7544 \end{bmatrix}, \\ \mathcal{V}_2 &= \begin{bmatrix} 0.1976 & 0 \\ 0 & 0.1976 \end{bmatrix}, M_1 = \begin{bmatrix} -4.6097 & -1.6175 \\ -1.5311 & -4.4893 \end{bmatrix}, \\ M_2 &= \begin{bmatrix} -0.0104 & -0.0007 \\ 0.0074 & -0.0460 \end{bmatrix}, M_3 = \begin{bmatrix} -2.2685 & -0.7267 \\ -0.7835 & -2.1632 \end{bmatrix}, \\ M_4 &= \begin{bmatrix} 0.0536 & -0.0085 \\ -0.0041 & 0.0501 \end{bmatrix}, M_5 = \begin{bmatrix} -2.2914 & -0.7143 \\ -0.8015 & -2.2272 \end{bmatrix}.\end{aligned}$$

The controller gain, $K_i = Y_i X_i^{-1}$. The values of X_i and Y_i , respectively,

$$X_1 = \begin{bmatrix} 0.0316 & -0.0054 \\ -0.0054 & 0.0395 \end{bmatrix}, X_2 = \begin{bmatrix} 0.7344 & 0.0132 \\ 0.0132 & 0.3848 \end{bmatrix},$$

$$Y_1 = \begin{bmatrix} 0.0418 & -0.0298 \\ -0.0062 & 0.2536 \end{bmatrix}, Y_2 = \begin{bmatrix} 1.4935 & 1.5079 \\ 0.0013 & 0.1489 \end{bmatrix},$$

Hence, the controller gain matrix K_i can be evaluated as:

$$K_1 = \begin{bmatrix} 1.2218 & -0.5854 \\ 0.9235 & 6.5433 \end{bmatrix}, K_2 = \begin{bmatrix} 1.9646 & 3.8517 \\ -0.0051 & 0.3871 \end{bmatrix},$$

with the above control gain, switching surface function (4) can easily achieve stochastic stability.

The first example with two-dimensional SNTSs, the simulation results are shown in Figures 3–8. Figure 3 shows the system's state responses, demonstrating that the proposed sampled-data controller successfully stabilizes the system. Figure 4 presents the control inputs $u_1(t)$ and $u_2(t)$, which are updated at non-uniform sampling instants. The switching behavior caused by Markovian modes is shown in Figure 5 showing random transitions between different states of the system. Figure 6 shows the responses of the sliding surface that converge to zero, demonstrating the robustness of the control design. The phase portrait shown in Figure 7 indicates that the state trajectories smoothly approach the equilibrium point, ensuring system stability. Finally, Figure 8 depicts the Brownian motion trajectories, representing stochastic disturbances acting on the system.

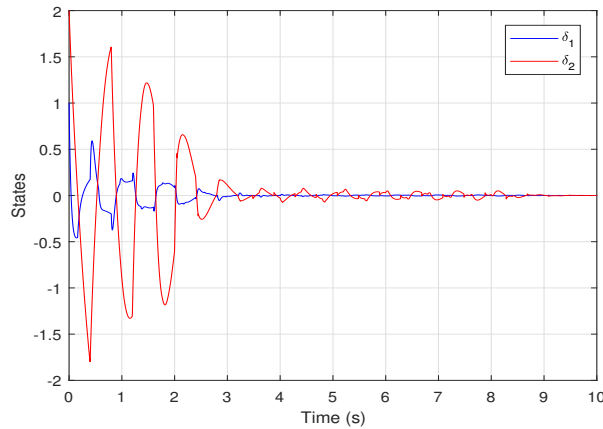


FIGURE 3. The state response curves of the system in Example 1

Example 2. A three-dimensional SNTSs (2) featuring two Markovian switching modes is analyzed, with the corresponding parameters specified as follows:

$$\hat{A}_1 = \begin{bmatrix} -1 & 0.3 & 0.2 \\ 0 & -2.0 & 0.4 \\ 0 & 0 & -1.5 \end{bmatrix}, \hat{A}_2 = \begin{bmatrix} -0.8 & 0.2 & 0.1 \\ 0 & -1.1 & 0.3 \\ 0 & 0 & -0.9 \end{bmatrix}, \hat{B}_1 = \hat{B}_2 = \begin{bmatrix} 1 & 0 & 0 \\ 0 & 1 & 0 \\ 0 & 0 & 1 \end{bmatrix},$$

$$\hat{C}_1 = \begin{bmatrix} 0.4 & 0.2 & 0.1 \\ 0.3 & 0.5 & 0.2 \\ 0.2 & 0.1 & 0.6 \end{bmatrix}, \hat{C}_2 = \begin{bmatrix} 0.2 & 0.3 & 0.1 \\ 0.1 & 0.4 & 0.2 \\ 0.3 & 0.2 & 0.5 \end{bmatrix}, \hat{D}_1 = \begin{bmatrix} 1.5 & 0.1 & 0.05 \\ 0.1 & 1.2 & 0.02 \\ 0.05 & 0.02 & 1.0 \end{bmatrix},$$

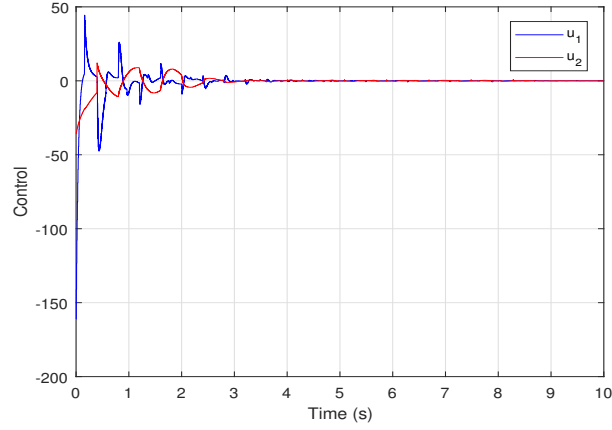


FIGURE 4. The control input responses of the system in Example 1

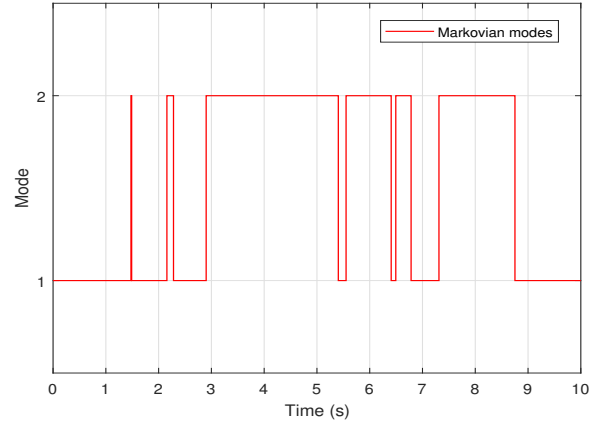


FIGURE 5. The system behavior involving jump modes in Example 1

$$\hat{D}_2 = \begin{bmatrix} 1.0 & 0.2 & 0.05 \\ 0.2 & 1.5 & 0.1 \\ 0.05 & 0.1 & 1.2 \end{bmatrix}, \hat{E}_1 = \begin{bmatrix} 0.2 & 0.05 & 0.05 \\ 0.05 & 0.2 & 0.05 \\ 0.05 & 0.05 & 0.2 \end{bmatrix}, \hat{E}_2 = \begin{bmatrix} 0.3 & 0.1 & 0.05 \\ 0.1 & 0.25 & 0.08 \\ 0.05 & 0.08 & 0.2 \end{bmatrix},$$

$$\hat{G}_1 = \begin{bmatrix} 0.01 & 0.005 & 0.002 \\ 0.005 & 0.01 & 0.003 \\ 0.002 & 0.003 & 0.01 \end{bmatrix}, \hat{G}_2 = \begin{bmatrix} 0.05 & 0.01 & 0 \\ 0.01 & 0.04 & 0.02 \\ 0 & 0.02 & 0.03 \end{bmatrix},$$

$$\hat{H}_1 = \begin{bmatrix} 0.02 & 0 & 0 \\ 0 & 0.015 & 0 \\ 0 & 0 & 0.01 \end{bmatrix}, \hat{H}_2 = \begin{bmatrix} 0.03 & 0.01 & 0 \\ 0.01 & 0.025 & 0.005 \\ 0 & 0.005 & 0.02 \end{bmatrix},$$

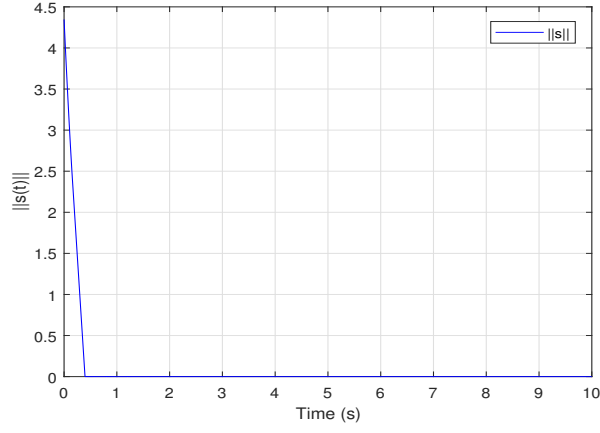


FIGURE 6. The behavior of the sliding surface for the system in Example 1

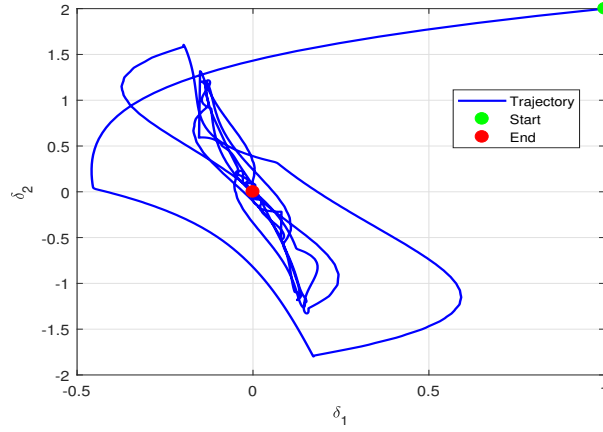


FIGURE 7. Phase Portrait in Example 1

when addressing the uncertainty terms, we present the matrix that incorporates the uncertainties, as shown below.

$$\hat{J}_{a1} = \begin{bmatrix} -0.01 & -0.005 & 0 \\ 0 & -0.01 & 0 \\ 0 & 0 & -0.01 \end{bmatrix}, \quad \hat{J}_{a2} = \begin{bmatrix} -0.02 & 0.01 & 0 \\ 0 & -0.015 & 0.005 \\ 0 & 0 & -0.01 \end{bmatrix},$$

$$\hat{J}_{b1} = \begin{bmatrix} -0.005 & -0.01 & 0 \\ 0 & -0.005 & 0 \\ 0 & 0 & -0.01 \end{bmatrix}, \quad \hat{J}_{b2} = \begin{bmatrix} -0.01 & 0.02 & 0 \\ 0 & -0.01 & 0.01 \\ 0 & 0 & -0.02 \end{bmatrix},$$

$$\hat{L}_1 = \hat{L}_2 = \begin{bmatrix} 1 & 0 & 0 \\ 0 & 1 & 0 \\ 0 & 0 & 2 \end{bmatrix},$$

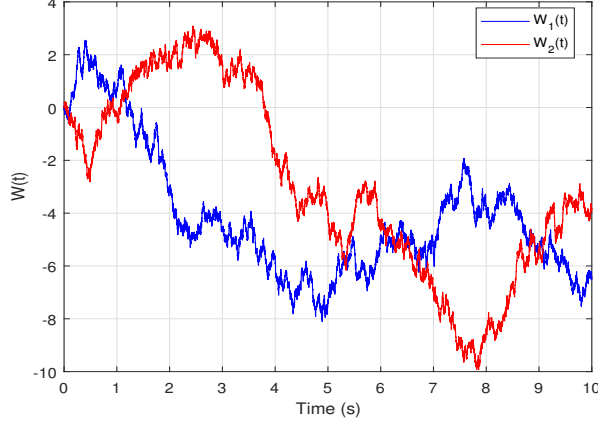


FIGURE 8. Wiener Process Trajectories (Brownian Motion) in Example 1

$$x_{11} = x_{12} = x_{21} \begin{bmatrix} 0.1 & 0 & 0 \\ 0 & 0.1 & 0 \\ 0 & 0 & 0.1 \end{bmatrix}, \quad x_{22} = \begin{bmatrix} 0.5 & 0 & 0 \\ 0.1 & 0.6 & 0 \\ 0 & 0.2 & 0.7 \end{bmatrix},$$

where x_{1i} and x_{2i} are the terms that arise in solving the trace terms.

$$\mathcal{H}_{11} = \begin{bmatrix} 0.5 & 0 & 0 \\ 0 & 0.4 & 0 \\ 0 & 0 & 0.3 \end{bmatrix}, \quad \mathcal{H}_{12} = \begin{bmatrix} 0.3 & 0 & 0 \\ 0 & 0.35 & 0 \\ 0 & 0 & 0.25 \end{bmatrix}, \quad \mathcal{H}_{13} = \begin{bmatrix} 0.3 & 0 & 0 \\ 0 & 0.35 & 0 \\ 0 & 0 & 0.25 \end{bmatrix},$$

$$\mathcal{H}_{21} = \begin{bmatrix} 0.4 & 0 & 0 \\ 0 & 0.4 & 0 \\ 0 & 0 & 0.4 \end{bmatrix}, \quad \mathcal{H}_{22} = \begin{bmatrix} 0.5 & 0 & 0 \\ 0 & 0.6 & 0 \\ 0 & 0 & 0.7 \end{bmatrix}, \quad \mathcal{H}_{23} = \begin{bmatrix} 0.3 & 0.1 & 0 \\ 0.2 & 0.3 & 0 \\ 0 & 0 & 0.4 \end{bmatrix},$$

the system time delay is taken to be $\tau = 0.6$, $\eta = 0.5$, $\dot{\eta} = 0.4$. The constants are

$$c = 0.2, \text{ and } k = \begin{bmatrix} 2 & 0 & 0 \\ 0 & 1.5 & 0 \\ 0 & 0 & 1.2 \end{bmatrix}.$$

Also, $h_p = 0.4$, $\pi = 0.3$, $\alpha = 0.1$, and $\gamma = 0.9$. Then, solving the LMI using MATLAB, we can get

$$P_1 = \begin{bmatrix} 0.1898 & -0.0123 & -0.0230 \\ -0.0123 & 0.0429 & -0.0318 \\ -0.0230 & -0.0318 & 0.0445 \end{bmatrix}, \quad P_2 = \begin{bmatrix} 1.2714 & 0.0482 & 0.0449 \\ 0.0482 & 1.2107 & 0.0933 \\ 0.0449 & 0.0933 & 1.2950 \end{bmatrix},$$

$$Q = \begin{bmatrix} 3.9633 & -0.0620 & -0.0355 \\ -0.0620 & 4.4547 & -0.1101 \\ -0.0355 & -0.1101 & 4.7022 \end{bmatrix}, \quad R = \begin{bmatrix} 3.4983 & 1.0359 & 0.7508 \\ 1.0359 & 4.8199 & 1.6414 \\ 0.7508 & 1.6414 & 5.7131 \end{bmatrix},$$

$$S = \begin{bmatrix} 1.9330 & -0.0439 & -0.0256 \\ -0.0439 & 2.0455 & -0.0690 \\ -0.0256 & -0.0690 & 2.1372 \end{bmatrix}, \quad T = \begin{bmatrix} 3.7600 & -0.1126 & -0.3109 \\ -0.1126 & 3.6838 & -0.3040 \\ -0.3109 & -0.3040 & 3.7738 \end{bmatrix},$$

$$\begin{aligned}
U &= \begin{bmatrix} 1.2890 & -0.0015 & -0.0010 \\ -0.0015 & 1.2862 & -0.0028 \\ -0.0010 & -0.0028 & 1.2835 \end{bmatrix}, \mathcal{V}_1 = \begin{bmatrix} 17.7154 & 0.9232 & 0.5457 \\ 0.9232 & 19.5917 & 1.4148 \\ 0.5457 & 1.4148 & 20.9335 \end{bmatrix}, \\
\mathcal{V}_2 &= \begin{bmatrix} 1.2001 & 0 & 0 \\ 0 & 1.2001 & 0 \\ 0 & 0 & 1.2001 \end{bmatrix}, M_1 = \begin{bmatrix} -9.8906 & -0.7321 & -0.4464 \\ -0.6891 & -11.1566 & -1.0964 \\ -0.4715 & -1.0917 & -12.0967 \end{bmatrix}, \\
M_2 &= \begin{bmatrix} 0.1843 & -0.0027 & -0.0014 \\ -0.0344 & 0.2255 & 0.0067 \\ -0.0205 & -0.0537 & 0.1958 \end{bmatrix}, M_3 = \begin{bmatrix} -4.9762 & -0.2706 & 0.0247 \\ -0.0952 & -5.4258 & -0.4000 \\ -0.1557 & -0.3556 & -5.7906 \end{bmatrix}, \\
M_4 &= \begin{bmatrix} 0.4319 & -0.0376 & -0.0391 \\ -0.0243 & 0.3248 & -0.0513 \\ -0.0517 & -0.0485 & 0.3311 \end{bmatrix}, M_5 = \begin{bmatrix} -4.6164 & -0.3187 & -0.2184 \\ -0.3264 & -5.1975 & -0.4960 \\ -0.2232 & -0.4908 & -5.5984 \end{bmatrix}.
\end{aligned}$$

The controller gain, $K_i = Y_i X_i^{-1}$. The values of X_i and Y_i , respectively,

$$\begin{aligned}
X_1 &= \begin{bmatrix} 0.2370 & 0.0134 & 0.0241 \\ 0.0134 & 0.2447 & 0.0209 \\ 0.0241 & 0.0209 & 0.2382 \end{bmatrix}, X_2 = \begin{bmatrix} 2.8938 & -0.1871 & -0.3248 \\ -0.1871 & 2.5003 & -0.3245 \\ -0.3248 & -0.3245 & 2.6782 \end{bmatrix}, \\
Y_1 &= \begin{bmatrix} 0.5493 & -0.0257 & 0.0310 \\ -0.0352 & 0.7070 & 0.0469 \\ 0.0103 & 0.0356 & 0.8276 \end{bmatrix}, Y_2 = \begin{bmatrix} 5.9300 & -0.9356 & -0.6703 \\ -0.9214 & 3.4071 & -0.6963 \\ -0.7239 & -0.5792 & 4.6348 \end{bmatrix},
\end{aligned}$$

hence, the controller gain matrix K_i can be evaluated as:

$$K_1 = \begin{bmatrix} 2.3390 & -0.2258 & -0.0861 \\ -0.3104 & 2.9081 & -0.0270 \\ -0.3056 & -0.1380 & 3.5177 \end{bmatrix}, K_2 = \begin{bmatrix} 2.0310 & -0.2263 & -0.0314 \\ -0.2471 & 1.3275 & -0.1291 \\ -0.0577 & -0.0125 & 1.7220 \end{bmatrix}.$$

The second example with three-dimensional SNTSs, Figures 9–14 present the corresponding results. Figure 9 shows that the state responses remain stable under the proposed controller. Figure 10 displays the control inputs updated at non-uniform sampling instants. The Markovian switching among modes is shown in Figure 11 reflecting the stochastic behavior of the system. Figure 12 demonstrates that the sliding surfaces converge to zero, confirming the robustness of the control law. The phase portrait in Figure 13 illustrates smooth trajectories converging to equilibrium, and Figure 14 shows the Brownian motion trajectories representing random noise influences on the system dynamics.

8. Conclusion. This paper has presented a robust H_∞ SDSMC strategy for SNTSs affected by nonlinearities, mixed time delays, parameter uncertainties, Lévy noises, and Markovian switching. By designing an integral SMS and a corresponding SDSMC law, we established sufficient conditions for the second moment exponential stability of the closed-loop system. The proposed approach uses a carefully constructed LKF, the generalized Itô formula, and advanced inequality techniques to derive stability criteria and ensure H_∞ performance. Furthermore, the dynamics of the sampled-data sliding mode system were analyzed, and the resulting stability criterion guarantees robust performance against stochastic jumps and modeling uncertainties. Finally, numerical simulations have validated the effectiveness and robustness of the proposed control strategy. Future work will focus on extending the proposed framework to output-feedback and observer-based control designs, as well as incorporating actuator saturation and input constraints under Lévy noise

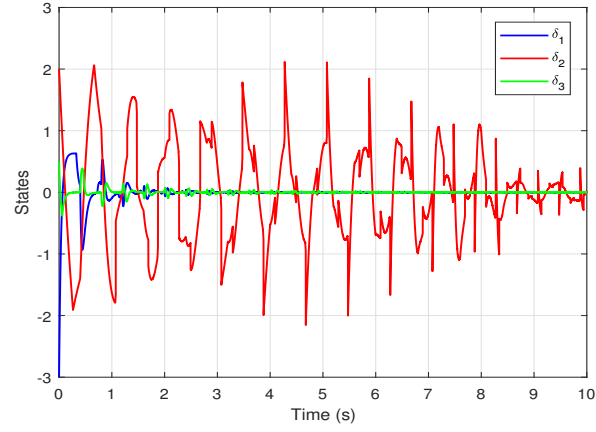
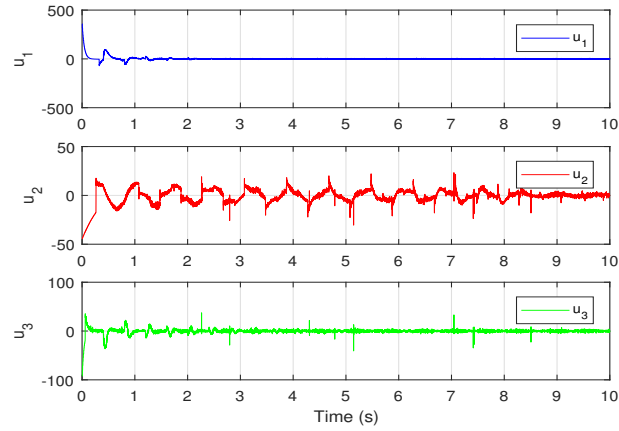


FIGURE 9. State trajectories of the system in Example 2

FIGURE 10. Responses of the control inputs $u_i(t)$ in Example 2

disturbances. In addition, event-triggered or adaptive sampling mechanisms may be investigated to further reduce communication and computational burdens. Experimental validation on real-world stochastic systems affected by Lévy noise is also an important direction for future research.

Author contributions. All authors contributed equally and significantly to the writing of this article and typed, read and approved the final manuscript.

Availability of data and materials. Data sharing does not apply to this article as data sets were not generated or analyzed during the current study.

Competing interests. The authors declare that they have no competing interests.

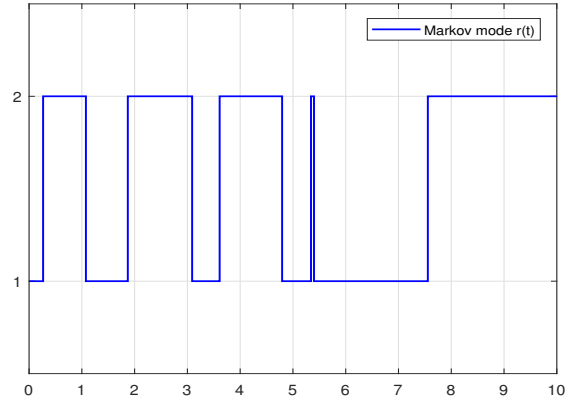


FIGURE 11. The jumping modes in Example 2

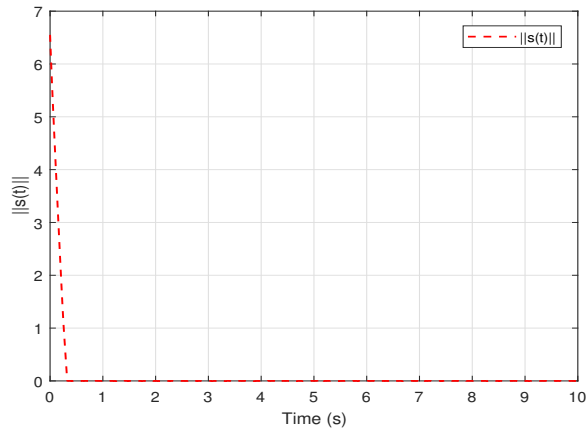


FIGURE 12. Responses of the sliding surface of the system in Example 2

REFERENCES

- [1] S. Ahmed, A. T. Azar and I. K. Ibraheem, [Nonlinear system controlled using novel adaptive fixed-time SMC](#), *AIMS Mathematics*, **9** (2024), 7895-7916.
- [2] Y. Altun, [Stability estimates for a class of neutral type systems with distributed time-varying delay components](#), *Advances in Continuous and Discrete Models*, **2025** (2025), 1.
- [3] T. S. Amer, T. A. Bahnasy, H. F. Abosheiaha, A. S. Elameer and A. Almahalawy, [The stability analysis of a dynamical system equipped with a piezoelectric energy harvester device near resonance](#), *Journal of Low Frequency Noise, Vibration and Active Control*, **44** (2025), 382-410.
- [4] Z. Cao, Z. Wang, Y. Niu, J. Song and H. Liu, [Sliding mode control for sampled-data systems subject to deception attacks: Handling randomly perturbed sampling periods](#), *IEEE Transactions on Cybernetics*, **53** (2022), 7034-7047.
- [5] Z. Cao, Z. Wang, J. Song and Y. Niu, [Sliding-mode control for sampled-data systems over fading channels: Dealing with randomly switching sampling periods](#), *IEEE Transactions on Automatic Control*, **69** (2023), 3190-3197.

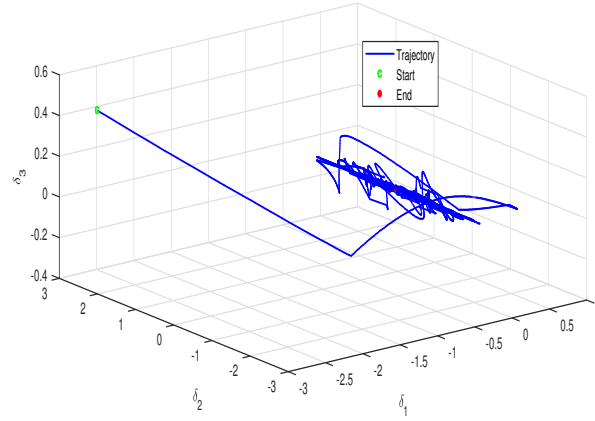


FIGURE 13. Phase Portrait in Example 2

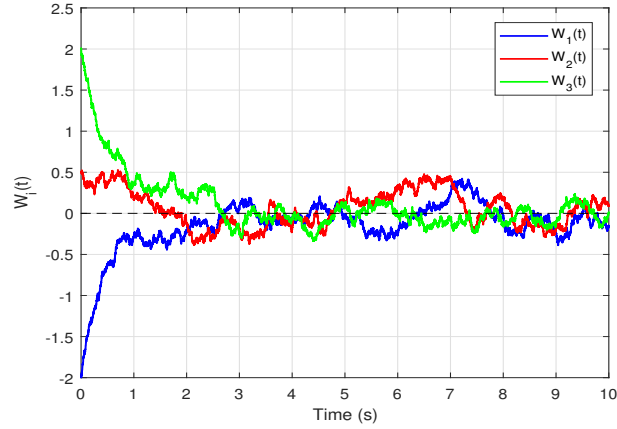


FIGURE 14. Wiener Process Trajectories (Brownian Motion) in Example 2

- [6] H. Chen, P. Shi and C. C. Lim, [Exponential synchronization for Markovian stochastic coupled neural networks of neutral-type via adaptive feedback control](#), *IEEE Transactions on Neural Networks and Learning Systems*, **28** (2016), 1618-1632.
- [7] Q. Chen, D. Tong, W. Zhou and Y. Xu, [Adaptive exponential state estimation for Markovian jumping neural networks with multi-delays and Lévy noises](#), *Circuits, Systems, and Signal Processing*, **38** (2019), 3321-3339.
- [8] Q. Chen, D. Tong, W. Zhou, Y. Xu and J. Mou, [Exponential stability using sliding mode control for stochastic neutral-type systems](#), *Circuits, Systems, and Signal Processing*, **40** (2021), 2006-2024.
- [9] G. Cheng and H. Shen, [Adaptive event-triggered asynchronous finite-time \$H_\infty\$ filter design for linear neutral semi-Markovian jumping systems with mixed sensor faults](#), *International Journal of Robust and Nonlinear Control*, **35** (2025), 3700-3714.
- [10] C. Duan and M. Tian, [Event-triggered synchronization control of uncertain neutral-type neural networks with time-varying delays and actuator saturation](#), *IEEE Access*, **12** (2024), 17571-17581.

- [11] C. Ge, B. Wang, X. Wei and Y. Liu, [Exponential synchronization of a class of neural networks with sampled-data control](#), *Applied Mathematics and Computation*, **315** (2017), 150-161.
- [12] L. Huang and X. Mao, [SMC design for robust \$H_\infty\$ control of uncertain stochastic delay systems](#), *Automatica*, **46** (2010), 405-412.
- [13] X. Huang and Y. Ma, [Sampled-data sliding mode exponential synchronisation of Master-Slave Markovian jump complex networks with nonlinear perturbation](#), *International Journal of Systems Science*, **51** (2020), 1714-1732.
- [14] Y. Jia and J. Yang, [Stochastic stability and stabilization of Markov jump linear systems with fixed dwell time and unknown transition rates](#), *2022 34th Chinese Control and Decision Conference (CCDC)*, IEEE, (2022), 3332-3338.
- [15] Y. Kao, J. Xie, C. Wang and H. R. Karimi, [A sliding mode approach to \$H_\infty\$ non-fragile observer-based control design for uncertain Markovian neutral-type stochastic systems](#), *Automatica*, **52** (2015), 218-226.
- [16] C. Li, X. Xu and M. Liu, [The stochastic fixed-time synchronization of delays neural networks driven by Lévy noise](#), *Systems & Control Letters*, **190** (2024), 105839.
- [17] Y. Li, B. Kao, J. Xie and Y. Kao, [A guaranteed cost approach to dynamic output feedback control for neutral-type Markovian jumping stochastic systems](#), *Journal of Systems Science and Complexity*, **34** (2021), 1487-1500.
- [18] P. Lin, F. Deng, X. Zhao, F. Wan and Y. Huang, [Stability analysis of networked stochastic systems with time delays under deception attacks by Sampled-data control](#), *IEEE Transactions on Systems, Man, and Cybernetics: Systems*, **55** (2025), 2950-2960.
- [19] Q. Luo, Y. Gong and C. Jia, [Stability of gene regulatory networks with Lévy noise](#), *Science China Information Sciences*, **60** (2017), 072204.
- [20] X. Mao, *Stochastic Differential Equations and Applications*, Elsevier, 2007.
- [21] T. Nguyen, C. Edwards, V. Azimi and W. C. Su, [Improving control effort in output feedback sliding mode control of sampled-data systems](#), *IET Control Theory & Applications*, **13** (2019), 2128-2137.
- [22] B. Øksendal, *Stochastic Differential Equations*, Springer, 2003.
- [23] W. Qi, G. Zong and H. R. Karimi, [Observer-based adaptive SMC for nonlinear uncertain singular semi-Markov jump systems with application to DC motor](#), *IEEE Transactions on Circuits and Systems I: Regular Papers*, **65** (2018), 2951-2960.
- [24] W. Qi, G. Zong and H. R. Karimi, [SMC for nonlinear stochastic switching systems with quantization](#), *IEEE Transactions on Circuits and Systems II: Express Briefs*, **68** (2021), 2032-2036.
- [25] P. Shi, F. Li, L. Wu and C. C. Lim, [Neural network-based passive filtering for delayed neutral-type semi-Markovian jump systems](#), *IEEE Transactions on Neural Networks and Learning Systems*, **28** (2017), 2101-2114.
- [26] K. Sobczyk, *Stochastic Differential Equations: With Applications to Physics and Engineering*, Springer Science & Business Media, 2013.
- [27] J. Sun, J. Chen, G. P. Liu and D. Rees, [On robust stability of uncertain neutral systems with discrete and distributed delays](#), *2009 American Control Conference*, IEEE, 2009, 5469-5473.
- [28] N. M. Thoiyab, M. Fazly, R. Vadivel and N. Gunasekaran, [Stability analysis for bidirectional associative memory neural networks: A new global asymptotic approach](#), *AIMS Mathematics*, **10** (2025), 3910-3929.
- [29] D. Tong, Q. Chen, W. Zhou, J. Zhou and Y. Xu, [Multi-delay-dependent exponential synchronization for neutral-type stochastic complex networks with Markovian jump parameters via adaptive control](#), *Neural Processing Letters*, **49** (2019), 1611-1628.
- [30] D. Tong, C. Xu, Q. Chen, W. Zhou and Y. Xu, [Sliding mode control for nonlinear stochastic systems with Markovian jumping parameters and mode-dependent time-varying delays](#), *Nonlinear Dynamics*, **100** (2020), 1343-1358.
- [31] F. X. Wang, J. Q. Cui, J. Zhang, Y. F. Lu and X. G. Liu, [Stabilization of fractional nonlinear systems with disturbances via sliding mode control](#), *International Journal of Robust and Nonlinear Control*, **35** (2025), 202-221.
- [32] S. Wen, T. Huang, X. Yu, M. Z. Q. Chen and Z. Zeng, [Aperiodic sampled-data sliding-mode control of fuzzy systems with communication delays via the event-triggered method](#), *IEEE Transactions on Fuzzy Systems*, **24** (2015), 1048-1057.
- [33] Z. G. Wu, P. Shi, H. Su and J. Chu, [Sampled-data exponential synchronization of complex dynamical networks with time-varying coupling delay](#), *IEEE Transactions on Neural Networks and Learning Systems*, **24** (2013), 1177-1187.

- [34] C. Xu, M. Farman, A. Shehzad and K. Sooppy Nisar, [Modeling and Ulam–Hyers stability analysis of oleic acid epoxidation by using a fractional-order kinetic model](#), *Mathematical Methods in the Applied Sciences*, **48** (2025), 3726-3747.
- [35] X. Yang, T. Zhao and Q. Zhu, [Aperiodic event-triggered controls for stochastic functional differential systems with sampled-data delayed output](#), *IEEE Transactions on Automatic Control*, **70** (2024), 2090-2097.
- [36] X. Yang, Q. Zhu and H. Wang, [Exponential stabilization of stochastic systems via novel event-triggered switching controls](#), *IEEE Transactions on Automatic Control*, **69** (2024), 7948-7955.
- [37] J. Yuan, C. Zhang and T. Chen, [Command filtered adaptive neural network synchronization control of nonlinear stochastic systems with lévy noise via event-triggered mechanism](#), *IEEE Access*, **9** (2021), 146195-146202.
- [38] D. Zeng, R. Zhang, S. Zhong, J. Wang and K. Shi, [Sampled-data synchronization control for Markovian delayed complex dynamical networks via a novel convex optimization method](#), *Neurocomputing*, **266** (2017), 606-618.
- [39] H. B. Zeng, K. L. Teo, Y. He and W. Wang, [Sampled-data stabilization of chaotic systems based on a T–S fuzzy model](#), *Information Sciences*, **483** (2019), 262-272.
- [40] J. Zhang and E. Fridman, [Improved derivative-dependent control of stochastic systems via delayed feedback implementation](#), *Automatica*, **119** (2020), 109101.
- [41] M. Zhang and Q. Zhu, [Stabilization of unstable impulsive systems via stochastic discrete-time feedback control with Lévy noise](#), *Nonlinear Analysis: Hybrid Systems*, **56** (2025), 101585.
- [42] H. Zhou, Y. Zhang and W. Li, [Synchronization of stochastic lévy noise systems on a multi-weights network and its applications of chua’s circuits](#), *IEEE Transactions on Circuits and Systems I: Regular Papers*, **66** (2019), 2709-2722.
- [43] J. Zhou, T. Cai, W. Zhou and D. Tong, [Master–slave synchronization for coupled neural networks with markovian switching topologies and stochastic perturbation](#), *International Journal of Robust and Nonlinear Control*, **28** (2018), 2249-2263.
- [44] L. Zhou, Q. Zhu, Z. Wang, W. Zhou and H. Su, [Adaptive exponential synchronization of Multislave time-delayed recurrent neural networks with Lévy noise and regime switching](#), *IEEE Transactions on Neural Networks and Learning Systems*, **28** (2017), 2885-2898.
- [45] Q. Zhu, [Asymptotic stability in the \$p\$ th moment for stochastic differential equations with Lévy noise](#), *Journal of Mathematical Analysis and Applications*, **416** (2014), 126-142.
- [46] Q. Zhu, [Event-triggered sampling problem for exponential stability of stochastic nonlinear delay systems driven by Lévy processes](#), *IEEE Transactions on Automatic Control*, **70** (2025), 1176-1183.

Received January 8, 2026; revised February 17, 2026; early access March 13, 2026.